



# The MAPP Outrigger Technical Proposal

Version 1.1

B. Acharya<sup>1,2</sup> J. Alexandre<sup>1</sup> P. Benes<sup>3</sup> B. Bergmann<sup>3</sup> S. Bertolucci<sup>7</sup> A. Bevan<sup>4</sup> R. Brancaccio<sup>16</sup> H. Branzas<sup>5</sup> P. Burian<sup>3</sup> M. Campbell<sup>6</sup> S. Cecchini<sup>7</sup> Y. M. Cho<sup>8</sup> M. de Montigny<sup>9</sup> J. Ellis<sup>1</sup> M. Fairbairn<sup>1</sup> D. Felea<sup>5</sup> M. Frank<sup>10</sup> J. Hays<sup>4</sup> A. M. Hirt P.Q. Hung<sup>12</sup> J. Janecek<sup>3</sup> M. Kalliokoski<sup>13</sup> D. Lacarère<sup>6</sup> C. Leroy<sup>14</sup> G. Levi<sup>7</sup> A. Maselek<sup>27,28</sup> A. Margiotta<sup>7,16</sup> A. Maulik<sup>7,9</sup> N. Mauri<sup>7</sup> N. E.Mavromatos<sup>1,17</sup> M. Mieskolainen<sup>18</sup> L. Millward<sup>4</sup> V. A. Mitsou<sup>15</sup> G. Moss<sup>19</sup> Musumeci<sup>15</sup> I. Ostrovskiy<sup>20</sup> P.-P. Ouimet<sup>21</sup> J. Papavassilou<sup>15</sup> L. Patrizzii<sup>7</sup> G. E. Pāvāļš<sup>5</sup> J. L. Pinfold<sup>9,1</sup> L. A. Popa<sup>5</sup> V. Popa<sup>5</sup> M. Pozzato<sup>7</sup> S. Pospisil<sup>3</sup> A. Rajantie<sup>21</sup> R. Ruiz de Austi<sup>15</sup> Z. Sahnoun<sup>7,23</sup> M. Sakellariadou<sup>1</sup> K. Sakurai<sup>28</sup> S. Sarkar<sup>1</sup> G. Semenov<sup>24</sup> A. Shaa<sup>9</sup> G. Sirri<sup>7</sup> K. Sliwa<sup>7</sup> R. Soluk<sup>9</sup> M. Spurio<sup>7</sup> M. Staelens<sup>9</sup> M. Suk<sup>3</sup> M. Tenti<sup>25</sup> V. Togo<sup>7</sup> J. A. Tuszynski<sup>9</sup> A. Upreti<sup>20</sup> V. Vento<sup>7</sup> O.Vives<sup>7</sup>

<sup>1\*</sup>Theoretical Particle Physics & Cosmology Group, King's College London, UK.

<sup>2\*</sup>International Centre for Theoretical Physics, Trieste, Italy .

<sup>3</sup>IEAP, Czech Technical University in Prague, Czech Republic .

<sup>4</sup>School of Physics and Astronomy, Queen Mary University of London, London, England .

<sup>5</sup>Institute of Space Science, Bucharest - Măgurele, Romania .

<sup>6</sup>Experimental Physics Department, CERN, Geneva, Switzerland .

<sup>7</sup>INFN, Section of Bologna, Bologna, Italy .

<sup>8</sup>Asia Pacific Center for Theoretical Physics, Pohang, Korea .

<sup>9</sup>Physics Dept., University of Alberta, Edmonton, Alberta, Canada .

<sup>10</sup>Dept. of Physics, Concordia University, Montréal, Quebec, Canada .

<sup>11</sup>Dept. of Earth Sciences, Swiss Federal Institute of Technology, Zurich, Switzerland .

<sup>12</sup>Dept. of Physics, University of Virginia, Charlottesville, Virginia, USA .

<sup>13</sup>Physics Dept., University of Helsinki, Helsinki, Finland .

<sup>14</sup>Department of Physics, Concordia University, Montréal, Quebec, Canada .

<sup>15</sup>IFIC, Universitat de València - CSIC, València, Spain .

<sup>16</sup>Department of Physics & Astronomy, University of Bologna, Italy .

<sup>17</sup>National Technical University of Athens, Zografou Campus, Athens, Greece .

<sup>18</sup>Physics Dept., University of Helsinki, Helsinki, Finland .

<sup>19</sup>Track Analysis Systems Ltd, Bristol, UK .

<sup>20</sup>Physics Department, University of Alabama, Tuscaloosa, Alabama, USA .

<sup>21</sup>Physics Department, University of Regina, Regina, Saskatchewan .

<sup>22</sup>Physics Department, University of Regina, Regina, Saskatchewan .

<sup>23</sup>Centre for Astronomy, Astrophysics and Geophysics, Algiers, Algeria .

<sup>24</sup>Department of Physics, UBC, Vancouver, British Columbia, Canada .

<sup>25</sup>INFN, CNAF, Bologna, Italy

<sup>26</sup>Theoretical Physics Department, CERN, Geneva, Switzerland

<sup>27</sup>Laboratoire de Physique, Subatomique et de Cosmologie, Université Grenoble-Alpes  
CNRS/IN2P3, Grenoble France

<sup>28</sup>Institute of Theoretical Physics, University of Warsaw, Warsaw, Poland

\* **Communicating Author, E-mail: jpinfoldualberta.ca .**

## Abstract

This is the Technical Proposal for the outrigger detector for the MAPP (moEDAL Apparatus for Penetrating Particles) detector being installed in UA83 for data taking during Run-3 and on. The outrigger is an auxiliary detector designed to greatly improve the acceptance of the Phase-1 MAPP detector (MAPP-1) for milli-charged particles with large fractional charges. The outriggers are four 6m scintillator planks, comprised of 60 cm x 30 cm x 5 cm scintillator slabs, deployed in a horizontal duct joining the UA83 tunnel to the beam tunnel in the vicinity of the MAPP detector.

## 1 Introduction

A major part of the MoEDAL Collaboration’s physics program for LHC’s Run-3 and beyond involves the installation of a new detector called MAPP (MoEDAL Apparatus for Penetrating Particles) [1, 2]. MAPP’s purpose is to expand the physics reach of MoEDAL, that is focussed on the detection of Highly Ionizing Particle (HIP) avatars of new physics, to include the search for mini-charged particles<sup>1</sup> (mCPs) with charges as low as one thousandth the electron charge ( $e$ ) and weakly interacting very long-lived particle (LLPs) messengers of new physics. Thus the MoEDAL and MAPP detectors operating together will be able to detect: HIPs, mCPs and LLPs.

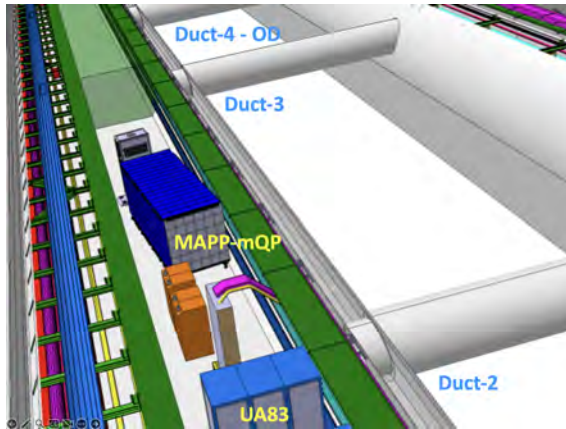
The MAPP outrigger detector is an array of scintillator blocks arranged in planks placed in a duct (Duct-4) joining the UA83 tunnel and the beamline tunnel, in the vicinity of the MAPP detector, as shown in Fig. 1. Its purpose is to significantly increase MAPP’s acceptance for feebly electromagnetically interacting particles with an effective charge greater than  $\sim 0.001e$ , where  $e$  is a single electric charge. This Technical Proposal describes the details of the design, construction and installation of the “Outrigger Detector.”

---

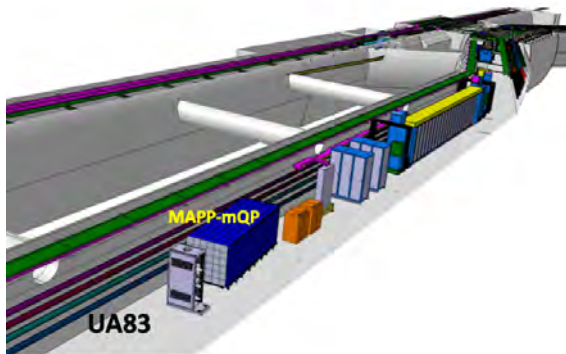
<sup>1</sup>We use the term mini-charged rather than milli-charged to denote the lightly ionizing particle as it does not imply that the charge is  $10^{-3}e$

## 2 The Outrigger Detectors for MAPP-1

The Phase-1 MAPP detector (MAPP-1) for LHC's Run-3 is currently being installed in UA83 tunnel some 100 m from the existing MoEDAL & LHCb detectors, to take data during LHC's Run-3. The MAPP-1 detector and its associated electronics rack has now been included in the overall LHC machine description as shown in Fig. 1. A drawing of the MAPP-1 detector is shown in Fig. 2. MAPP-1 is protected from Standard Model particles from interactions at IP8 by, on average, roughly 45m of rock and from cosmic rays by an overburden of approximately 110m of limestone.



(a)



(b)

**Fig. 1:** The deployment of the MAPP-mQP (MAPP-1) detector in UA83. The proposed Outrigger Detector (OD) deployment in Duct-4 is indicated.

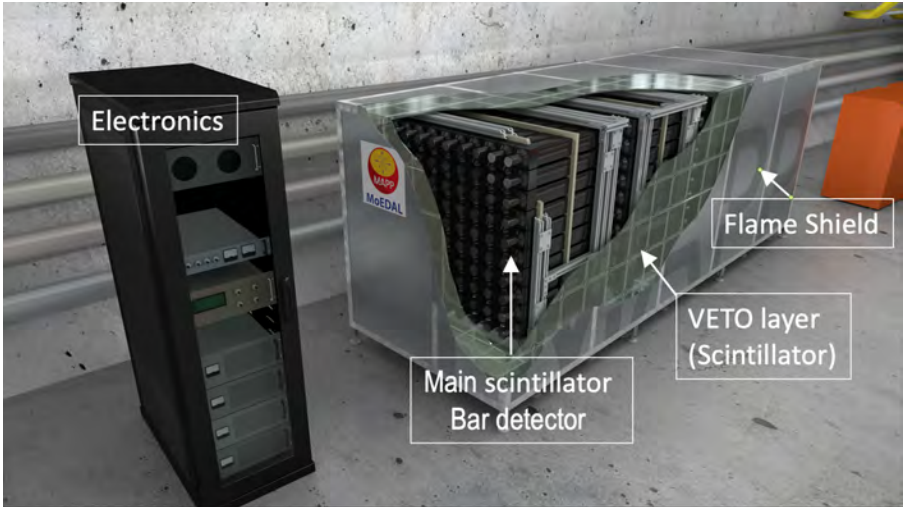


**Fig. 2:** A drawing of the MAPP detector showing the main elements of the MAPP detector.

The MAPP Phase-1 detector is designed to the search for mCPs. It is made up of four collinear sections, with sensitive cross-sectional area of roughly  $1.0 \text{ m}^2$ , each comprised of 100 ( $10 \text{ cm} \times 10 \text{ cm}$ ) plastic scintillator bars each 75cm long. Each bar is readout by one low-noise 3-inch PMT. The detector is arranged to point towards the IP. Thus, each through-going particle from the IP will encounter 3.0 m of scintillator and be registered by a coincidence of 4 PMTs. The 4-fold PMT coincidence essentially eliminates the background from "dark counts" in the PMTs. Additionally, the division of the detector into 4 bars virtually excludes all fake signal events arising from radiogenic backgrounds in the scintillator and PMTs. The MAPP-mCP "bar" detector is hermetically enclosed in a veto layer consisting of 1.25 cm thick scintillator plates read out by embedded scintillating fibre loops with a size of  $25 \text{ cm} \times 25 \text{ cm}$ .

### 3 Placement of the Outrigger Detectors

Initially, Duct-3 adjacent to the MAPP-1 detector was chosen for the deployment of MAPP-1's 4-plane Outrigger detector. Ducts-1 and -2 were already carrying cables and were incorporated into the infrastructure of the LHC machine. Subsequent discussions with the LHC machine group revealed that Duct 3 would be reserved for future machine requirements. However, MoEDAL-MAPP has been given the green light to use Duct-4 for the Outrigger on approval of the project. The situation with Duct-5 is uncertain at this stage. The relative positions of Ducts 3,4 and 5 are shown in Fig. 3.

The effect on the sensitivity of the Outrigger due to its placement in the Ducts is shown in Fig. 4. The physics process used to make this determination

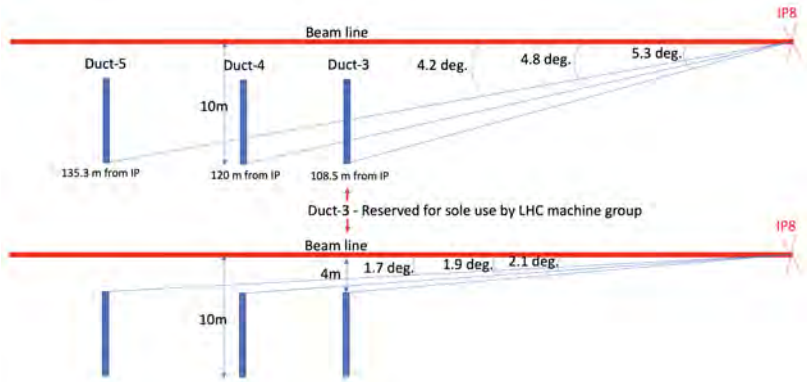


**Fig. 3:** The deployment of the Outtrigger Detectors adjacent to the MAPP-1 detector. Duct-3 has been reserved for machine use. Duct-4 is available to deploy Outtrigger Detectors. The situation with Duct-5 is uncertain at this point

is Drell-Yan production of mCPs, where four scintillator planes are placed in a single duct. As expected and as shown in Fig. 4 the sensitivity is best for Duct-3 the most upstream Duct, very slightly worse for Duct-4, and slightly worse again for Duct-5. However, the actual duct chosen does not make a significant difference to the sensitivity achieved with the Outtrigger detector, as indicated in Fig. 4.

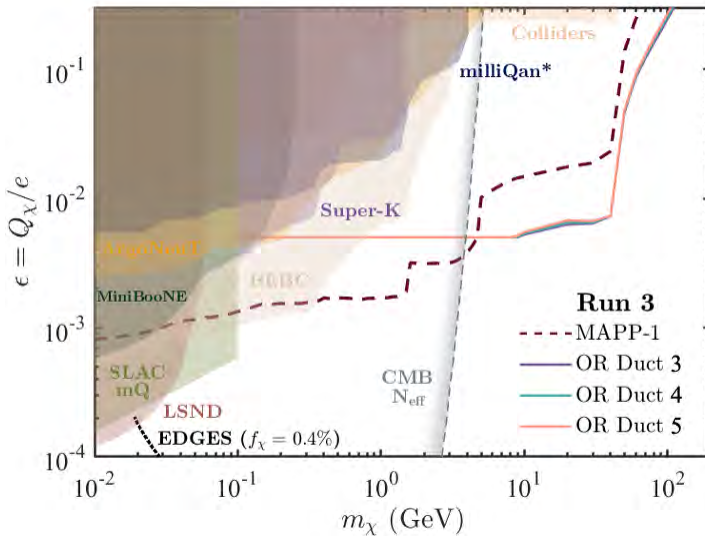


**Fig. 4:** The effect on sensitivity of the Outtrigger Detector for mCPs due to its position.

The fact that the increased distance of the Outrigger from IP8, owing to its deployment in the Duct-4, had little effect is because the increased distance is only  $\sim 10\%$  of its original placement distance in Duct-3. Also, the greater distance places the detector at slightly smaller angle to the beamline, allowing us to accrue some enhanced acceptance arising from the kinematics of the production process.

### 3.1 Outrigger Detector Technology

The basic scintillator unit of the Outrigger Detector is shown in Fig. 5. It is comprised a block of acrylic scintillator (Bicron BC-412 ) of size 60 cm x 30 cm x 5 cm readout through a light guide by a single 3.5-inch low noise PMT (HZC Photonics XP82B2FNB) <sup>2</sup> This unit is assembled on a frame with another unit for insertion on a rail into the Duct that houses the Outrigger Detectors. This subdivision is chosen to facilitate manual handling. The units are held at an angle of  $45^\circ$  in order that the path length of particles from the IP in the scintillator is increased from 5cm to approximately 7 cm.

The scintillator detectors are installed as basic subunits, shown in Fig. 6 in Duct-4 joining the UA83 tunnel to the beam tunnel. The numbering of Ducts starts from the end of UA83 nearest to IP8. Four scintillator layers are inserted into Duct-4, as shown in Fig. 7. For example, a requirement for a gold-plated milli-charged particle candidate would be the coincidence of all 4 layers where the scintillator blocks responding would be those consistent with a track passing through the Outrigger Detectors.

Typically, a Minimum ionizing particle will lose around 1 to 2 MeV/cm in a good plastic scintillator and generate of the order of 10K to 20K photons per MeV lost. Consequently, this particle will deposit a comparatively large amount of light, of the order  $1.4 \times 10^5$  photons in each scintillator block through which the muon passes. Assuming a quantum efficiency of 25% for the detecting PMT and a 50% efficiency for the photon reaching the PMT We have estimated that the light collection efficiency, including the loss due to photo-cathode efficiency, is  $\sim 10\%$ .

Roughly, a relativistic charged particle ionizes according to the square of its charge a particle with around  $10^{-2}e$  would give approximately 14 photons in each slab, giving us of the order of one (PE). Thus, using this very approximate calculation the blocks are limited to the measurement of mCPs with a charge of  $20^{-2}e$  and above. However, several other factors need to be taken in account including a detailed knowledge of the photon detection efficiency of each bar as well as factors that effect the particle by particle emission of scintillation light that depends on such factors as the charge, the velocity and Landau-Vavilov fluctuations [4] in energy loss. Indeed, at the limit of the sensitivity of the detector the most probable energy loss instead of the average energy loss is required.

A detailed simulation dealing with all of the above-mentioned details is required especially when for small enough values of fractional charge the

---

<sup>2</sup>The HZC Photonics PMT is functionally the same as the HZC XP82B20D [3]

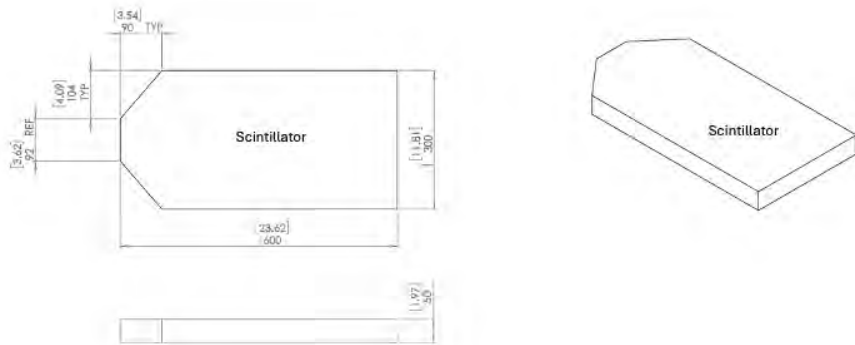


**Fig. 5:** The basic 5 cm thick plastic scintillator (Bicron 412) slab from which the Outrigger Detector is comprised is readout by a single 3.5-inch HZC Photonics (XP82B2FNB) PMT.

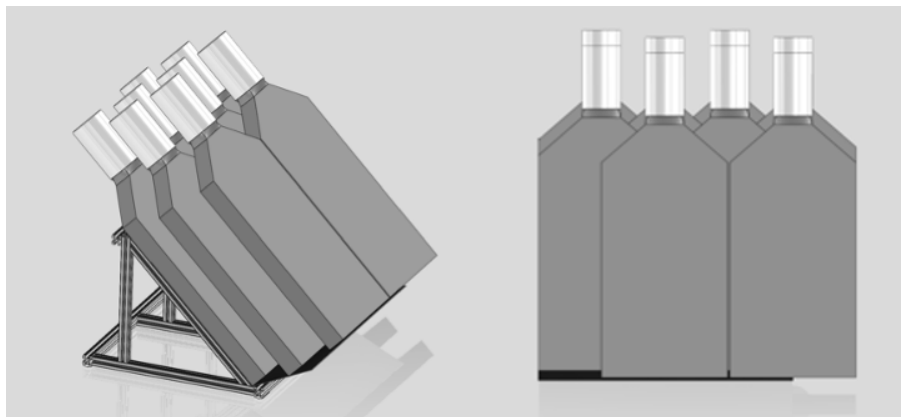


**Fig. 6:** The installation subunit of the outrigger detector.

expected number of photons produced per MCP passing through the detector is less than one, pushing the limitations of the outrigger detector. Such a simulation named SUMMA (Simulation of the UA83, MoEDAL, MAPP-mCP Arena) has been created and is under test.

### 3.2 HV, Readout, DAQ, Calibration and Trigger

The PMT used in the readout of the scintillator bars is a HZC Photonics P82B2FNB PMT Tube. The High Voltage divider will be resistive with an impedance of  $4M\Omega$  a maximum voltage of 2000V and a current of  $500\mu A$ . The photocathode will be at ground potential with positive high voltage applied to the anode. The signal will be capacitively coupled to the cable.



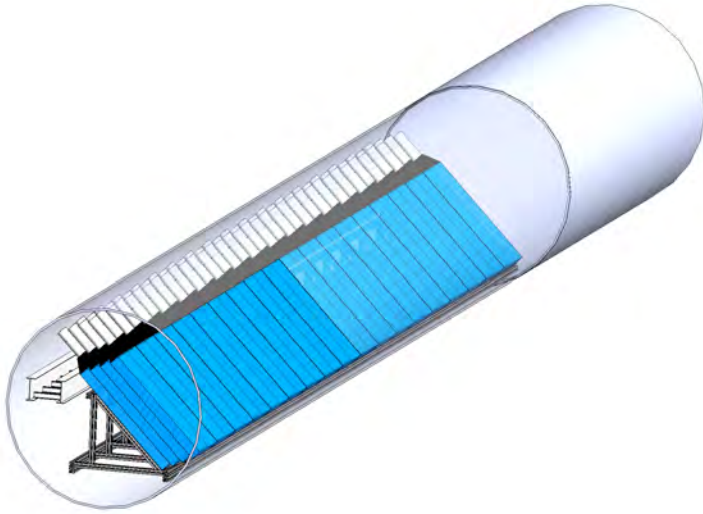


**Fig. 7:** The deployment of the Outrigger Detector in Duct-4. Note that in this depiction 2m of concrete shielding is shown. It has been recently determined that only one metre of iron shielding will be utilized allowing more detector to be installed.

The power supply will consist of a boost converter to convert from 48Vdc to 250V using a coupled inductor to reduce the maximum voltage seen by the controller. Several stages of a Cockcroft-Walton multiplier will then increase this up to 2000V. The boost converter will be controlled by a small inexpensive 6 pin microcontroller which can accept serial data and synchronization pulses from the DAQ. The Front end is connected to the DAQ via an MCX connector. Power, signal and control will all be delivered via the same cable to reduce cabling costs. In this way we avoid HV cables and connectors as well as the related safety concerns.

The technology for HV, readout, DAQ, calibration, and trigger used for the main MAPP-1 detector will also be used for the Outrigger Detector. However, the Outrigger will have its own software trigger and operate autonomously, although the data will use the same DAQ computers and data-path out of the cavern.

A block diagram of the electronic readout and powering scheme for the MAPP and Outrigger Detectors is shown in Fig. 8. Each DAQ board will consist of 32 identical channels. The DAQ will connect to the front end via an MCX connector. A bias tee will couple the 48V dc supply to the signal line. Control signals for the high voltage power supply will also be coupled capacitively to the signal line. The amplifier chain will include a programmable gain amplifier to allow tuning of the overall system gain, minimal shaping and an anti-alias filter. The ADC will consist of a Texas Instruments ADS4249 dual



channel amplifier running at 240MHz, and 14bit readout to an Intel (formally Altera) Cyclone IV FPGA via LVDS.

The FPGA will perform discrimination, coincidence and peak detection of the incoming signals, with inter-fpga communication via backplane B-LVDS. Events that pass both the software trigger and the veto will be passed for storage via Ethernet to the PC(s). The system will run synchronously to the LHC (bunch crossing) clock, The orbit clock will also be veto background events from non-colliding bunches and to synchronize health keeping events and switching regulator noise to the abort gap.

Normally the data will be transferred via 1 Gbit/s ethernet link to an external computer. There will also be a computer in UGC1 that will take data if there is a failure in the ethernet connection. The data will be sent via the onsite storage via the internet to analysis sites in Canada, UK, USA, Spain and Italy. The 19 readout boards will be housed directly underneath the MAPP-mQP detector, in the UGC1 gallery.

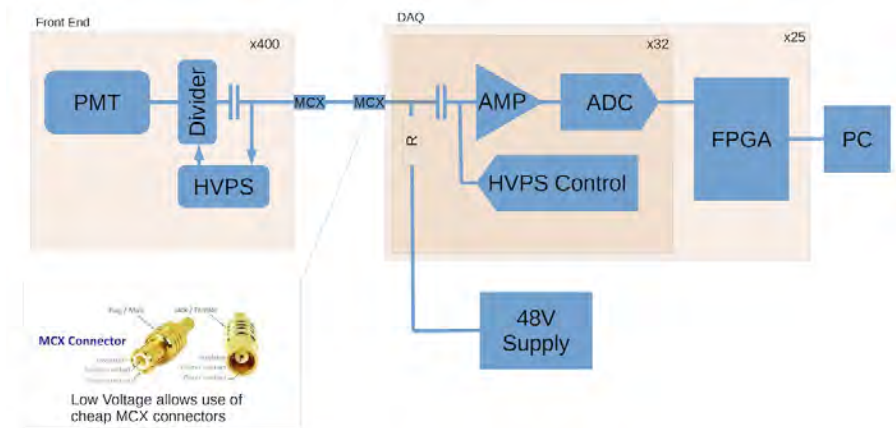


**Fig. 8:** A block diagram showing the basic electronics readout structure for the MAPP-mQP detector,

The data rate is expected to be on average less than 1 Hz from each of the 400 bars of the MAPP main detector with around another 200 channels from the veto detectors and radiator at maximum. There are 80 extra channels contributed by the Outrigger Detector, corresponding to the 80 scintillator blocks comprising the detector.

Conservatively assuming a rate of, on average, 1 Hz for each of the 680 channels involved, with 200 bits per channel (or PMT pulse) being read out, the total data rate is around 140 Kbits/sec. Our system can read out 4 million channels/s, 5900 times more capacity than needed. The data in the front-end readout electronics is pipe-lined, so that large fluctuations up in the data rate can be handled. Thus, these boards could be used for high luminosity LHC.

There will be a number of software triggers carried out by FPGAs housed in the readout system. The trigger philosophy is to widen the trigger as much as possible. Additionally, we aim to take minimum bias events at the rate of approximately 5% of the total data rate. Nevertheless, we expect the amount of data readout will be somewhat less than the maximum mentioned just above. Further, higher-level ‘triggers’, will be applied offline to the raw data. We chose to adopt the philosophy of utilizing a very broad software trigger, rather than reading out the complete detector at each beam crossing since the flow of data through the various triggers enables us to monitor the physics response of our detector online.

An example of an important ‘software’ trigger for MAPP-1 and the Outrigger Detectors, is the through going muon-trigger. In this case the muon would pass through all four scintillator blocks pointing at the IP as well as the photon tagging boards (that can also serve as VETO detectors) that sandwich the main scintillator detector sections. In the MAPP-1 case a basic muon trigger is formed from a coincidence of 4 contiguous scintillator sections.

In the case of the Outrigger Detector, the muon trigger is formed by a ‘hit’ in each of the four scintillator layers where those hits are consistent with forming a collinear track. The efficiency trigger efficiency to be very near 100%.

### **3.2.1 The Outrigger Detector Calibration System**

Like the MAPP-1 detector the Outrigger Detector will be calibrated in two main ways. The first method utilizes an array of blue LED’s emitting at the peak of the wavelength sensitivity of the scintillator slabs forming the Outrigger Detector. Each scintillator slab is equipped with a LED which is pulsed in such a way as to mimic the light deposited by particles with varying fractional charge, down to the level where only single photoelectrons are being detected by the PMTs.

The second calibration method employs the small flux of high-momentum muons from IP8. Characteristically, these muons will be minimum ionizing particles (MIPs). We can simulate the light emission of a fractionally charged particle by inserting a neutral density filter between the PMT and the scintillator slab. The transmittance of the filter would be chosen to reduce the amount of light entering the PMT from the muon by the same amount that a fractionally charged particle would have reduced ionization compared to a MIP. This ‘absolute’ calibration is transferred to the LED system by comparison of the signal generated by the calibration LED in the PMT to the signal obtained when a neutral density filter is interposed.

We aim to have a small number of slabs equipped with filters during data taking in order to check the calibration over time using muons from the interaction point. The filters can be moved/removed manually during shutdowns. Calibration transfer studies will be carried out using neutral density filters corresponding to particles with several different mini-charges, down to a charge of 0.01e. We expect to be able to interpolate between these points to obtain an understanding of the calibration across the sensitive range, using the LEDs.

The daily LED calibration will be performed with a number of different pulse times and voltages corresponding to particles with different ionizations.

## 4 Beam Induced Radiation Backgrounds in the MAPP-1 Region of the UA83 Tunnel

A prototype MAPP-mQP detector was deployed during 2018 in UGC1. Its main purpose was to enable us to estimate the data rate we would expect during RUN-3. The prototype was comprised of nine 10 cm x 10 cm x 120 cm scintillator bars deployed in a *horizontal* configuration in the UGC1 gallery. Each bar was read out at both ends by a PMT. A hit on a scintillator bar was counted if the PMTs at each end of the bar registered a coincident signal above the threshold. We observed that with beam-off each bar was hit at around a rate  $\sim 0.05$  Hz. This rate was largely due to cosmic rays, despite the roughly 100m rock overburden. This level of cosmic background was consistent with our GEANT-4 based simulations. We expect this level of cosmic ray activity in the UA83 tunnel as it lies at approximately the same depth beneath the same rock overburden.

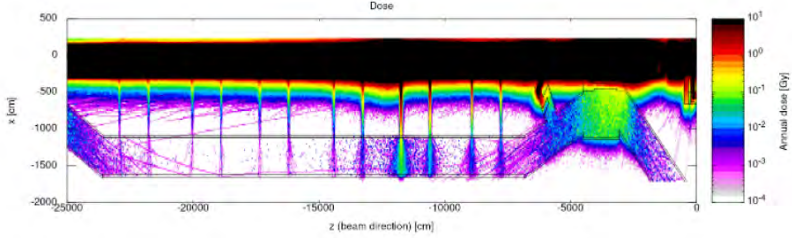
When the beam was turned on we observed the rate in the MAPP-mQP prototype bars increased by a factor of 4 to 5. According to the FLUKA studies presented in the above subsection on beam-induced radiation backgrounds in the MAPP-mCP region of the UA83 tunnel, the beam-induced backgrounds in the MAPP-mCP detector in UA83 should be considerably less than expected in UGC1, except in the regions where Ducts connect UA83 with the beam tunnel.

To study beam induced backgrounds more fully Francesco Cerutti and Alessia Ciccotelli of the Beam-Machine Interaction section of the CERN Engineering Department have performed a study of the beam induced backgrounds in the UA83 tunnel and the UGC1 gallery using the FLUKA Monte Carlo program, assuming an annual luminosity of  $10 \text{ fb}^{-1}$  [5].

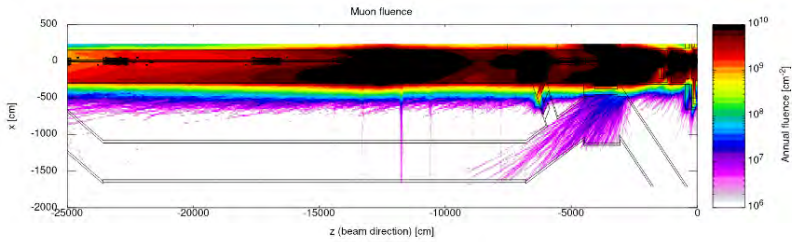
A critical issue is the effect of the radiation on the detector and on its electronic readout system. A key variable here is the dose which is shown in Fig. 9. As can be seen from Fig. 9 the dose received by the MAPP-mCP detector in its new position in the UA83 tunnel is estimated to be below 1mGy/year, a factor of 300 less than its initially proposed deployment in the UGC1 gallery.

Fig. 10 shows a map of the muon fluence component of beam-induced backgrounds expected at the UA83 ( $< 10^6 \text{ cm}^{-2}$ ) and UGC1 ( $\sim 3 \times 10^8 \text{ cm}^{-2}$ ) locations of the MAPP-mCP detector. We see a better than a 300 times reduction of the muon flux in the UA83 location compared to the UGC1 position.

Likewise the neutron flux ( $5 \times 10^7/\text{year}$ ) and photon flux ( $10^8 \text{ cm}^{-2}/\text{year}$ ) at the position of the MAPP-mCP detector in UA83 show at least a few hundred times reduction over MAPP-mCP's previously proposed position in the UGC1 gallery, as shown in Fig. 11 and Fig 12, respectively.



**Fig. 9:** The dose rate in the vicinity of MAPP-1. The top map shows the UGC1 gallery and the bottom map shows the UA83 tunnel.



**Fig. 10:** The muon fluence in the vicinity of MAPP-1. The top part of map shows the UGC1 gallery and the bottom map shows the UA83 tunnel.

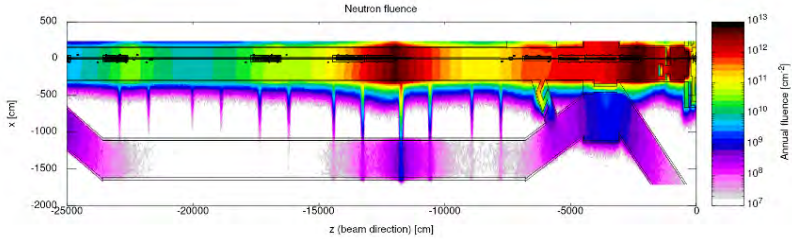


**Fig. 11:** The neutron fluence in the vicinity of MAPP-1. The top part of the map shows the UGC1 gallery and the bottom map shows the UA83 tunnel.

#### 4.1 Beam and Cosmic Backgrounds in the Vicinity of the Outrigger

In the region by the mouth of the Ducts in the UA83 tunnel, the beam-induced backgrounds rise substantially, since radiation can travel down the Ducts unimpeded. Thus, before we install the outrigger detectors in Duct-4 we will install shielding in the beam-tunnel side of the Duct.

As discussed previously we are required by the Machine Group to use Duct-4 and to use iron pieces rather than poured concrete as shielding. We worked

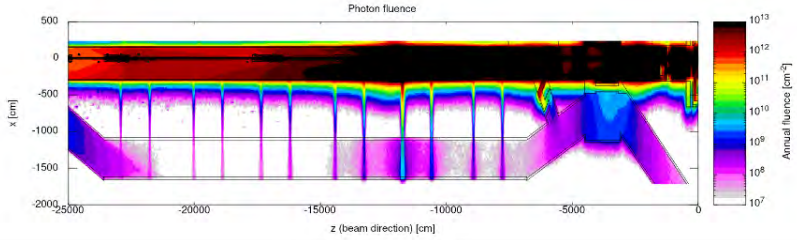


**Fig. 12:** The photon fluence in the vicinity of MAPP-1. The top part of the map shows the UGC1 gallery and the bottom map shows the UA83 tunnel.

with the Beam-Machine Interaction section of the CERN Engineering Department to assess the effect of the shielding using FLUKA simulations. In this estimate, we established that 1m of continuous iron shielding was equivalent to 2m of poured (continuous) concrete. The effect of Total Ionizing Dose (TID) of 1m of continuous iron shielding is shown in Fig. 13.

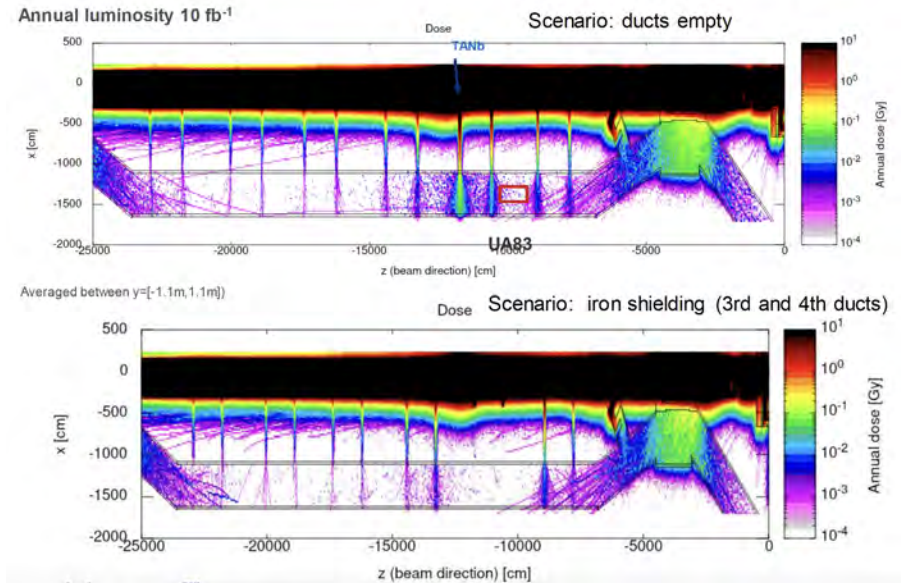


**Fig. 13:** The map of TID in the MAPP-1 region of UA83.

As can be seen from Fig. 13 the 1m of iron shielding substantially reduced the passage of radiation through Ducts 3 and 4, where the 1m of continuous iron shielding was deployed. This is despite the presence of TANb nearly adjacent to the mouth of Duct-4. Fig. 14 shows the effect of the shielding on the Thermal Neutron Flux (TNF).

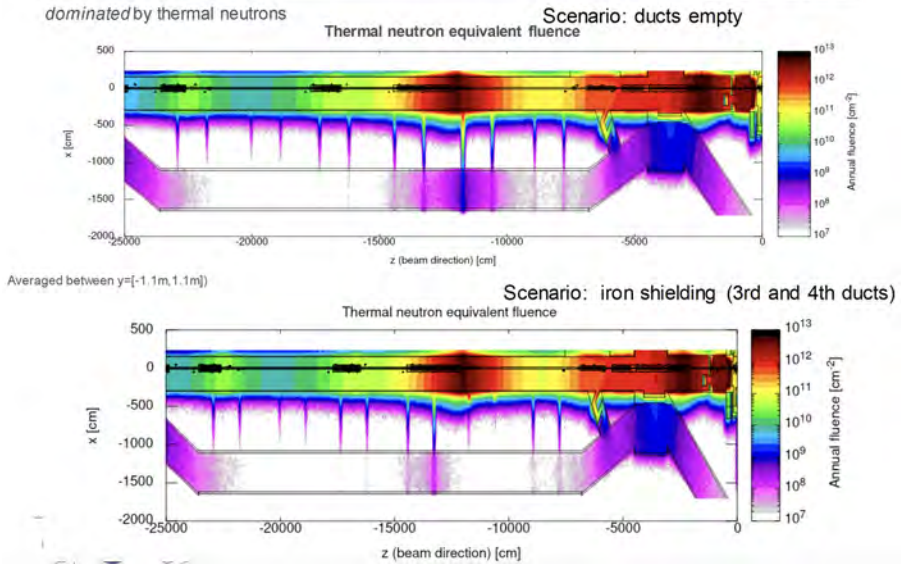


**Fig. 14:** The map of the TNF in the MAPP-1 region of UA83.

The effect of the shielding on the fluences of High Energy Hadrons (HEH), thermal neutrons, Dose, photons and muons is shown in Fig. 15. In the plots depicted the 1m of continuous iron shielding is compared with 2m of poured concrete.

## 4.2 Cosmic Backgrounds

A prototype MAPP-mQP detector was deployed during 2018. Its main purpose was to enable us to estimate the data rate we would expect during RUN-3. The prototype was comprised of nine 10 cm x 10 cm x 120 cm scintillator bars deployed in a *horizontal* configuration in the UGC1 gallery. Each bar was readout at both ends by a PMT. A hit on a scintillator bar was counted if the PMTs at each end of the bar registered a coincident signal above threshold. We observed that with beam-off each bar was hit at around a rate  $\sim 0.05$  Hz. We assumed that this rate was largely due to cosmic rays, despite the roughly 100m rock overburden. This level of cosmic background was consistent with our GEANT-4 based simulations. We expect this level of cosmic ray activity in the UA83 tunnel as it lies at the same depth beneath the same rock overburden.

## 5 Construction and Installation of the Outrigger Detector and Extra Shielding

The detector will be constructed and tested at the University of Alberta and at the University of Alabama, although the detectors comprising the initial



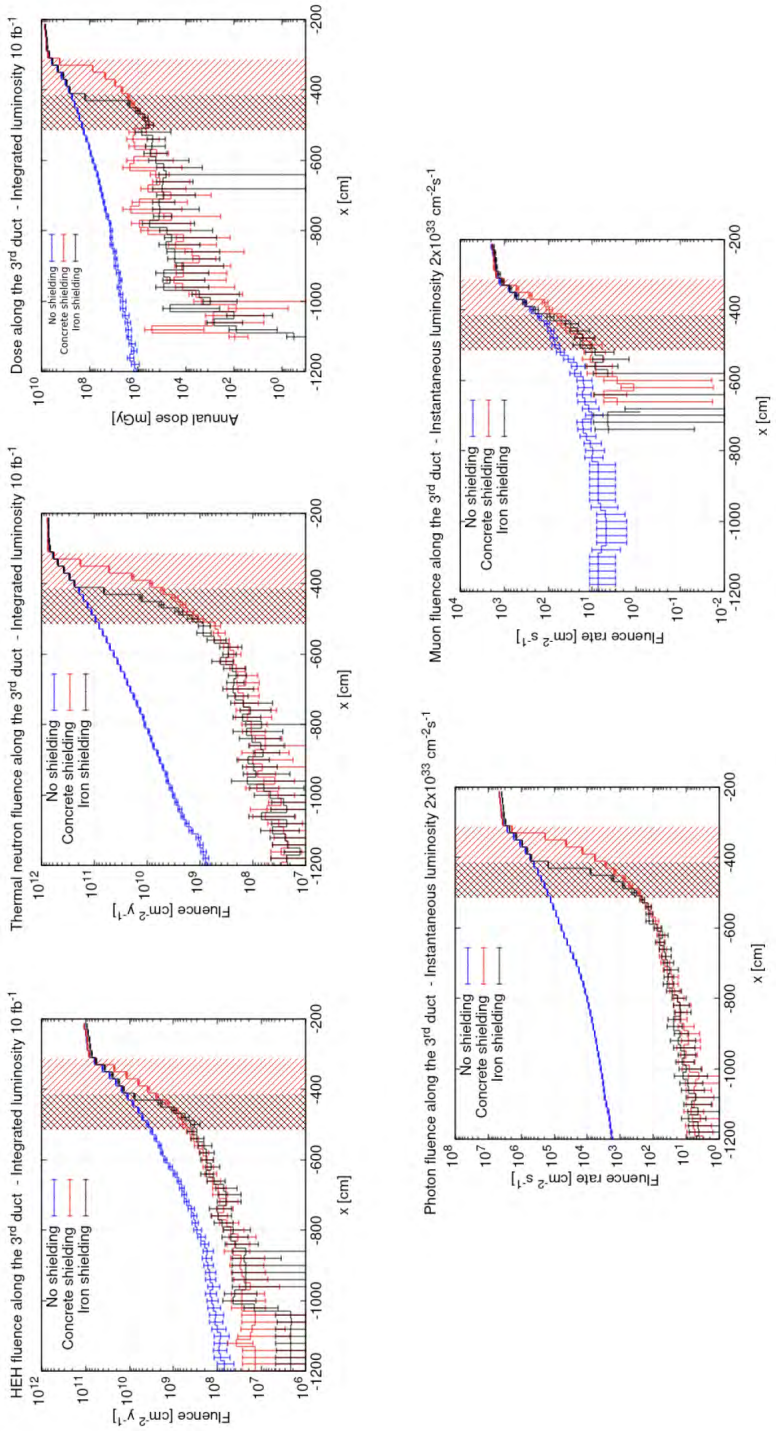


**Fig. 15:** The effects of 1m of continuous iron shielding and 2m of poured concrete shielding on beam backgrounds in Ducts 3 & 4 in the MAPP-1 region.



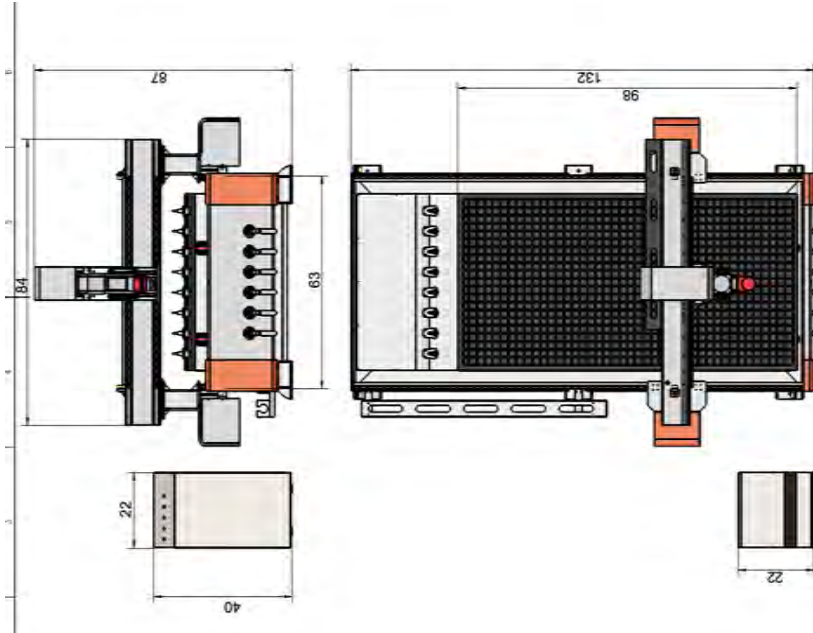


**Fig. 16:** A plan view of the the PERFORMA ATC PLUS router and cutter manufactured by PRECIX, featuring a 4 ft x 8 ft bed .

deployment of detectors in 2024 will all be fabricated at the University of Alberta.

A main element of the construction schedule is the installation of a new machine tool to fabricate the scintillator blocks. A plan drawing of the machine, the PERFORMA ATC PLUS router and cutter manufactured by PRECIX, featuring a 4 ft x 8 ft bed is shown in Fig. 16. This machine is scheduled to be installed in the first half of December 2024.

If the outrigger project is approved the first elements to be installed in Duct-4 will be the support rails for the Outrigger detector, the cable trays and the iron shielding.

In the above-mentioned simulation of the protection afforded by iron and concrete shielding against beam backgrounds only continuous shielding was considered. As the Machine Group has ruled out the possibility of poured concrete we are limited to iron shielding. The iron shielding will be inserted into the duct in pieces. These pieces will be of different lateral sizes in order to pack the circular space of the duct as efficiently as practically possible. A diagram showing the packing scheme is shown in Fig. 18.

Although the shielding packing scheme is efficient it will be impossible to eradicate narrow holes between the shielding pieces. The effect of the non-uniform shielding will be studied by initially deploying one of two Outrigger Detector installation subunits worth of detectors plus neutron dosimeters attached to various thicknesses of High-Density Polyethylene (HDPE) to study

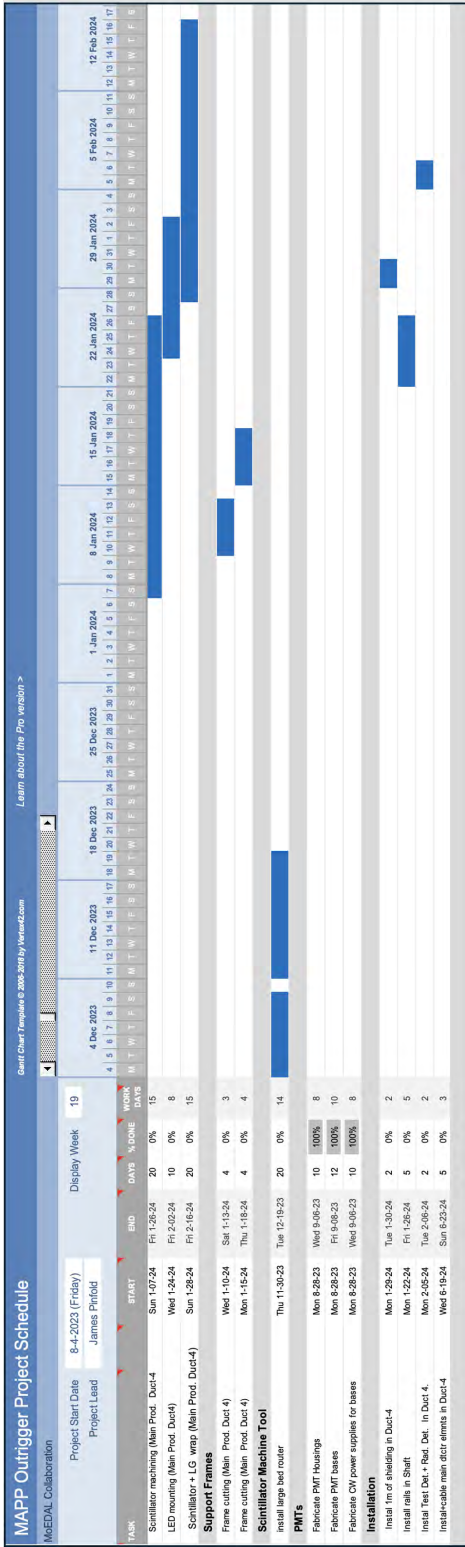
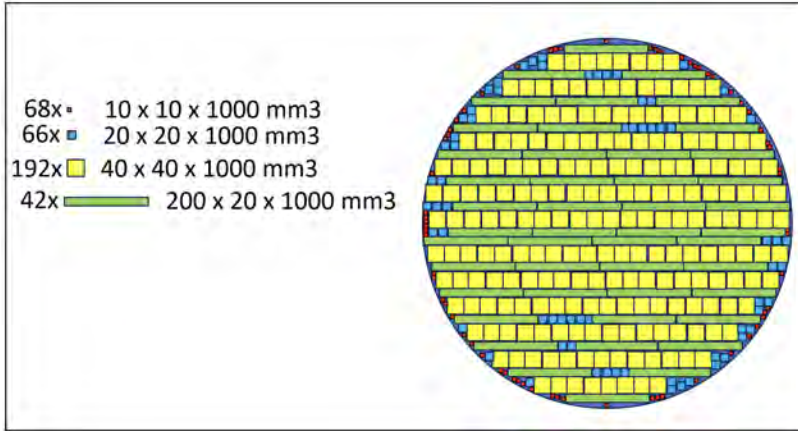


Fig. 17: schedule for the construction and installation of Outrigger Detector elements.



**Fig. 18:** The packing scheme for the 1m long iron elements constituting the shielding for the Outrigger detector in Duct-4.

the effectiveness of the shielding for data taking. After it has been shown that the shielding is adequate to enable efficient data taking, the full complement of detectors will be deployed.

The installation of this shielding was the topic of an Engineering Change Request: *MAPP Outrigger detector installation in UA83-LHC tunnel link ducts at LHC Pt 8*, submitted on the 19th of October 2023. This ECR, approved on November 1st 2023, is included in Appendix (A) [6]. If the MoEDAL-MAPP Outrigger Detector project is approved by the LHCC and CERN's Research Board, the installation of the iron shielding will go ahead in mid-January 2024. To enable ease of installation the shielding would be inserted from the beam-line tunnel side. The support rails and cable trays internal to the duct would be placed just before the shielding installation.

Here is an outline of the agreed installation schedule for the support rails, cable tray and shielding within Duct-4:

- Scaffolding will be installed on the LHC side W49:12/03-08/2023 (2 h)
- The team in charge of removing the air tightness plug on LHC side and the internal existing structure will work W50:12/10-15/2023 (2-3 days)
- The scan of the inside of the duct will take place end of W50 or W51 (1 h work)
- Duct-4 and region will be available for installation of our support rails and cable tray, internal to Duct-4, from W51:12/17-22/2023 till the end of W4:01/28/2024 (excluding Xmas break)
- The iron shielding will be laid W5:01/29/24 –j, 02/02/2024 (2 days)
- The air tightness plug will be re-installed in W6:02/5-11/2024 (0.5d)
- The scaffolding will be removed W6

Detectors can be inserted along the rail inside the duct, fully cabled. So we expect the installation of all additional detectors to be accomplished within a

day or two without the need to enter the duct. Thus, planned Technical Stops would adequately complete the task within the year. The scintillator detectors are installed as basic subunits, shown in Fig. 6. These units are inserted into Duct-4 along rails fixed on each side of the Duct. A total of 11 subunits (roughly 22 blocks wide) would be installed in Duct-4. The total area of plastic seen by particles from the IP as they impinge on Duct-4 is  $21 \times [30 \times 60 \times \sin 45^\circ] = 2.7 \text{ m}^2$ , compared to  $\sim 1 \text{ m}^2$  for the MAPP-1 detector.

The readout of the PMTs as well as the calibration system will be cabled into the main readout electronics readout rack of the MAPP detector as the Outrigger Detector installation subunits are installed. The electronics readout and calibration system is functionally the same as that of the MAPP-1 detector. The cables carrying LV power and signals to and from the PMTs are housed in the cable rack installed along the length of the Duct behind the scintillator blocks. Details of the installed detector are given in Fig. ?? and Fig. 7.

A Gantt chart showing the envisaged construction schedule is provided in Fig. 17. Note that all of the required power and readout electronics is now available.

The response of these detectors will be used to assess the efficacy of the shielding during the first weeks of data-taking in 2024. If the shielding is adequate, as we expect it to be, then we plan to install the remaining detectors in the first suitable Technical Stop. The modularization of the Outrigger Detector enables rapid installation, one Outrigger Detector installation unit at a time. We note that in 2023 there was 4 to 5 day TS at the end of June. This would be sufficient for us to complete the installation of the remaining detectors.

However, if it is determined the shielding needs some additional elements, we envisage it would be to reduce any flux of low energy neutrons propagating down the small channels between shielding elements, Our plan to deal with this eventuality would be to install HDPE layers between the Outrigger Detectors and the 1m iron plug, up to a thickness of 0.5 m. The exact thickness being determined from the neutron dosimeters installed with the test detectors. The installation of any additional shielding would take place in the YETS starting in 2024.

## 6 Safety Matters

The safety issues considered below arise from four sources, those to do with: the UA83 tunnel; the detector itself; and, detector operations. The approved Safety Derogation Request for the MAPP-1 detector which uses all the same detector elements as its Outrigger Detector is shown in Appendix (B) [7].

### 6.1 UA83 Tunnel and Detector Safety Issues

The UA83 tunnel is a full part of the LHC machine infrastructure with access via the PM85 lift directly to the floor of UA83. It is equipped with interlock access, smoke detector, fire alarms and forced ventilation.

The acrylic-based scintillator detector elements of the Outrigger are completely enclosed in the concrete Duct, in which they are housed. The total mass of plastic scintillator in Duct-4 is 400 kg. The safety sheets for acrylic plastic are included in Appendix (C).

The Outrigger Detectors are situated within Duct-4 that passes through the 8m thick concrete wall that separates the UA83 tunnel and the beam-line tunnel. Shielding is placed on the beamline tunnel side of Duct-4 to reduce beam backgrounds.. The remaining 7m of the Duct will be used to house the Outrigger Detector. Thus the Outrigger detectors are surrounded by metres of concrete, except for the opening into the UA83 tunnel. An aluminium flame shield will be placed across the mouth of the opening to completely isolate the detectors.

The MAPP/Outrigger detector electronics rack and MAPP detector will be monitored by an IR + Visible light digital camera placed in the vicinity of MAPP in the UA83 tunnel. The Outrigger detectors which do not obtrude into the UA83 tunnel itself are equipped with smoke and temperature detectors that are monitored in the same way as the MAPP-1 temperature sensors.

### **6.1.1 Safety Issues Related to the Readout Electronics & HV**

The readout electronics and power supplies are isolated and deployed up to 10m - 20m from the Outrigger Detectors in the electronics racks servicing the MAPP-1 detector. There are no HV cables or HV connectors as there is a “Cockcroft-Walton” type converter in the base of each PMT that converts LV power to HV power for the PMT. The power supplies are low voltage (24V), are current and temperature limited (turn off when current or temperature goes out of a predetermined range), and provide an alarm signal when current or voltage moves out of some predefined operating window. The MAPP-mQP and Outrigger detector electronics consume only 1800 watts of power.

All cabling is halogen-free according to the provisions in IS23 <sup>3</sup>. The only other heat source in the UA83 gallery arises from the MAPP-mQP detector electronics and amounts to only 1400 watts.

## **6.2 Safety Issues Relating to Detector Installation**

MAPP-1’s outrigger detector is designed to be installed in situ from pieces weighing a maximum of approximately 20 kgs each, although most elements will weigh substantially less. Thus the whole Outrigger detector can be taken underground using the machine side elevator at IP8. We envisage that a maximum of four people will need to be present in the UA83 gallery for installation of the MAPP Phase-1 detector. MoEDAL-MAPP’s installation personnel will, of course, be equipped with all the required safety gear and will operate according to the safety rules and guidelines described in the safety courses each team member will have taken and passed.

---

<sup>3</sup><https://edms.cern.ch/document/335745/4>

### 6.3 Safety Monitoring After Detector Installation

The MAPP-1 Outrigger detector is readout over ethernet through the same pathways as the MAPP-1 detector. It does not require a team to operate it during data taking. However, the detector must be monitored to ensure safe operation at all times. The safety systems that will be installed to ensure that the detector is operating safely are as follows:

- The power supplies are current limited. In addition, alarm conditions are defined that signal non-standard operating characteristics. The power supplies output and alarm conditions are monitored remotely with a feed supplied to the CERN Control Centre (CCC);
- Three temperature probes will be placed at the end, middle and entrance of Duct-4 housing the outrigger detector. Alarm conditions are defined that signal if any monitored temperature moves above normal ambient temperature in the UA83 tunnel. The temperature probe outputs and alarm conditions are monitored remotely with a feed supplied to the CCC.
- An IR camera will be installed on site to monitor the whole MAP-1 detector region. Again, the feed from the camera will be supplied to the CCC.

### 6.4 MoEDAL-MAPP Safety Organization

The MoEDAL-MAPP safety organization at CERN will be established before installation. It will consist of:

- An experimental Safety Officer (EXSO, formerly GLIMOS) as the point of contact for all experimental safety issues and communication with the EP Safety Office. The EXSO for MoEDAL for installation and the first year of running, will be the Technical Coordinator, Richard Soluk;
- Both the EXSO and the MoEDAL-MAPP Spokesperson will be available for urgent safety interventions required during the detector installation;
- All the activities of installation will be declared via IMPACT request [8] and analyzed via the usual work package analysis and VIC (Visite Inspection Commune) procedures ;
- The MoEDAL-MAPP safety files will be created on EP safety office EDMS and shared with the LHCb LEXGLIMOS.

### 6.5 Organization of Construction, Installation and Running of the Detector

The two bulleted lists below describe the basic organization of the construction and installation of the Phase-1 MAPP-mCP detector:

- **Project Managers:**
  - **MoEDAL Spokesperson** - James Pinfold;
  - **MoEDAL Technical Coordinator** - Richard Soluk;
  - **Chief engineer** - Mitchel Baker;

- **Chief electronics engineer + Trigger and DAQ coordinator** - Paul Davis;
  - **CERN based administrator** - Veronique Wedlake;
  - **CERN based liaison with Machine** - Francois Butin;
  - **EXSO(GLIMOS)** - Richard Soluk;
  - **Radiation Safety Officer** - Richard Soluk
- **Installation Crew**
    - Richard Soluk - Crew leader and responsible for mechanics installation;
    - Paul Davis - Readout electronics, power supplies and FPGA based trigger;
    - Aditya Upreti - General team member to assist in all aspects of installation;
    - Emanuela Musumeci - General team member to assist in all aspects of installation
    - Michael Staelens - General team member to assist in all aspects of installation
    - Mitch Kelly - General team member to assist in all aspects of installation
    - Phd-student/Post Doctoral student 1 - General team member to assist in all aspect of installation;
    - Phd-student/Post Doctoral student 2 - General team member to assist in all aspect of installation.

## 6.6 Staging and Temporary Storage Area

In order to facilitate the installation and operation of the Outrigger Detector the LHC machine side manager responsible for the allocation of surface space in the SBD building agreed that MoEDAL-MAPP Experiment can be temporarily attributed about 20 m<sup>2</sup> of surface space in SBD 2855, as indicated in the photograph in Fig. 19. This area will be used as buffer space for short-term storage of equipment before transport and installation underground, and for storing light tooling needed for assembly and installation. The zone will be cleared and fenced with mobile barriers and will be made available to the collaboration as of week-46 of 2021.

## 7 Maintenance and Operation of the Outrigger Detectors for MAPP-1‘ During Run-3

The MAPP-1 and Outrigger detector will be read out via ethernet during the run to large-scale onsite disk storage at CERN. The UA83 gallery is not accessible during LHC running periods. In the event of a failure or malfunction of the Outrigger Detector we will not be able to effect repair until we have a TS, or a YETS in which access to the UA83 tunnel is possible. Typically, there are a few Technical Stops (TSs) within the year besides the YETS.





**Fig. 19:** The temporary staging area in SBD 2855.

We could continue running with the failure of a large fraction of the readout channels although understandably this would compromise the physics performance of the detector. In order to reduce the risk of shutdown of data taking during the run we have included in our electronics design a redundant power supply system and a redundant DAQ computer, to ensure robust operation of the overall detector.

In order to continue data taking in the event of a disruption of the ethernet connection the DAQ server will have 60TB of local disk storage. Data will be written to this disk until the ethernet connection is re-established. During normal running the data rate will be well below 0.5 TB/day allowing an extended period of running without the need to export data to remote storage. Initially, the fewest possible restriction will be applied to the trigger and the data rate will be limited by storage write speeds.

The MAPP detector is designed to be operated remotely and to shut down if any MAPP-1 or MAPP-1 Outrigger power supply draws more than a set maximum current. Nevertheless, the MAPP-1 and Outrigger detectors need to be monitored 24/7 by personnel based on site primarily for safety purposes - as described in Subsection 6.4. This is achieved by having a team of at least two MoEDAL-MAPP physicists at CERN, full-time. So that at any time there is an on-call responsible while the machine is operating and during TSs. This team would be enhanced by an average of 0.5 FTE person, formed from MoEDAL-MAPP collaboration members who are visiting CERN and have the required safety training. For planned upgrades or maintenance during running periods, we will call on manpower resources described in Subsection 6.5.

## 7.1 The Outrigger Detector Control Centre

The base of operations of the MAPP detector is the MAPP Control Centre (MCC) in Bat. 17 R-007, the location of which is shown in Fig. 20. MAPP's CERN-based operators have access through their on-call cell phones to the monitoring and alarm system as well as simple controls that allow them to



**Fig. 20:** The location of the MAPP Control Room (Bat. 17 R-007).

turn off the power and alert the CCC. The on-call MAPP operator and the off-duty operator as well as the Technical Coordinator and Spokesperson also are connected to this system at all times via cellphone. During the day the on-call MAPP-1 Outrigger operator will usually sit in the control room. During the evening and night, the on-call will be connected by cell phone to the MAPP-1 and Outrigger control and monitoring services. The on-call cell phone will be switched on at all times.

## 8 Funding Plans for the MoEDAL-MAPP Phase-1 Installation

The MAPP-1 Outrigger detector has been made possible by contributions of equipment from other experiments. First, a long-term loan of scintillator from EXO-200 and a long-term loan for surplus HZC PMTs acquired for an eventually unfunded astroparticle physics experiment. We will use the same experimental facilities utilized by MAPP-1, including: electronic readout, DAQ, calibration and safety systems. The funding needed for extra readout boards, PMT bases, LED calibration units and power supplies will; be provided from MoEDAL-MAPP M&O funds, MoEDAL-MAPP-1's NSERC Discovery Grant; and, contributions from the UofA DUP funds. CERN has agree to cover the cost of the material for, and installation of, the 1m of iron shielding in Duct-4.

In terms of manpower, our project electronics engineer, mechanical engineer and detector technologist are funded from our existing NSERC MRS grant. We have sufficient funds in hand to deploy the Outrigger detector (as described above) to take data in Run-3.

## 9 Physics Issues

In order to fully understand the sensitivity of the MoEDAL-MAPP detector to we are performing studies of a number of relevant physics benchmarks.

Examples of initial benchmark studies are presented below. To complete these physics studies we need to fully and accurately simulate: the detector and its response; the passage of primary and secondary particles through the intervening infrastructure; and, the transport of cosmic ray particles through the 105 m overburden. The complete Simulation package UA83-MAPP-MoEDAL Arena (SUMMA) is discussed below.

## 9.1 The Full Simulation of the UA83, MoEDAL, MAPP-mCP Arena (SUMMA)

The previous version of SUMMA, with the MAPP-mCP detector deployed in the UGC1 region, was nearing completion in Spring of 2021 when the decision was made to move MAPP's location to the UA83 tunnel. The move required an extensive update to the SUMMA code to take into account the MAPP-mCP new final position 100m away (UA83) from the IP. Additionally, the modeling of the intervening infrastructure had to be completely redone. However, the existing cosmic ray simulation module of SUMMA did not require extensive updates.

The SUMMA simulation is derived from: the final CAD drawings of the MAPP-mCP detector; accurate CAD drawings of the machine infrastructure; and, the existing model of cosmic ray transport through the overburden. In all, the simulation involves over 2500 elements. The SUMMA code will be ready for use in mid-December 2021.

The Physics Processes included in SUMMA, are:

- Primary Interaction and secondary particles, factory lists :
  - FTFP\_Bert model of hadronic showers
  - QGSP\_BERT\_HP for neutron fluxes
- Transportation and Decay;
- Electromagnetic Interactions.
  - Gamma conversion, Compton scattering, photo-electric effect for gammas;
  - Multiple scattering, ionization, bremsstrahlung for electrons and annihilation for a positron;
  - Multiple scattering, ionization, bremsstrahlung and pair production for muons;
  - Multiple scattering and ionization for other particles.
- Scintillation processes
  - Scintillation and Cerenkov for particles;
  - Absorption, Rayleigh scattering, Mie scattering and boundary processes for optical photons.

The SUMMA ionization energy loss calculation for milli-charged particles is partially based on the approach adopted in the References [9, 10].

## 9.2 Mini-Charged Particles from Dark QED - a Physics Benchmark

An initial study of the sensitivity of the MAPP-1 Outrigger detector to mCPs is given in Fig. 21. We here consider a class of Feebly Interacting Particle (FIP) that has a mini-charge (mCP) as small as  $10^{-3}e$ , or lower. A common scenario is from a Dark Sector model where one considers a mCP coupled through a very light kinetically mixed dark photon [11][12]. Although the mCP does not carry SM electroweak quantum numbers it behaves as a particle with a tiny electric charge. The DY process provides the main production channel for GeV-range mCPs at the LHC. The sensitivity of the MAPP-mCP detector deployed at UA83 to mini-charged particles produced in this way is shown in Fig. 21.

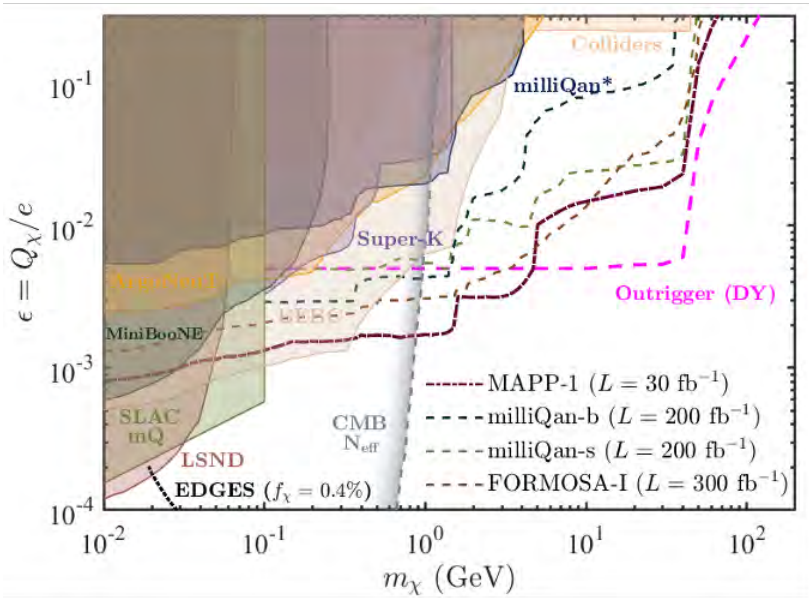


**Fig. 21:** Direct bounds from accelerator-based searches and indirect bounds from the effective number of neutrinos from Planck are shown. The projected sensitivity for mCPs, for models with a massless dark photon, are presented for milliQan, MAPP-mCP and FORMOSA-1 at Run-3. The existing bounds given here are described in more detail in Ref [13, 14].

We consider here a class of Feebly Interacting Particle (FIP) that has a mini-charge (mCP) as small as  $10^{-3}e$ , or lower. A common scenario is from a Dark Sector model where one considers a mCP coupled through a very light kinetically mixed dark photon [11][12]. Although the mCP does not carry SM electroweak quantum numbers it behaves as a particle with a tiny electric charge. The DY process provides the main production channel for GeV-range

mCPs at the LHC. The sensitivity of the MAPP-mCP detector deployed at UA83 to mini-charged particles produced in this way is shown in Fig. 21.

Beside DY production, the channels included in our analysis, include the pair production of mini-charged particles from the decays of the  $\Upsilon$ ,  $J/\psi$ ,  $\psi(2S)$ ,  $\phi$ ,  $\rho$ , and  $\omega$  as well as Dalitz decays of the  $\pi^0$ ,  $\eta$ ,  $\eta'$ , and  $\omega$ .

It should be noted that in Fig. 21 the detector efficiency *has* been modelled for the MAPP-bar detector but not for the Outtrigger [14]. Backgrounds have not been taken into account in both cases. We expect the limits that we can place on the DY production of mini-charged particle pairs to soften slightly when this is done, in the near future. As can be seen from Fig. 21, the MAPP-mCP is highly competitive with other mCP search experiments, especially at high masses.

### ***Backgrounds***

A potential source of background mentioned previously is the dark count from the PMT. For the HZC-phonics, the dark count rate is typically 600 cps. Considering the mCP trigger, that consists of requiring an mCP signal in 4 collinear blocks in coincidence, with a trigger window of 25 ns and a beam crossing rate of 40 MHz, we would expect a trigger rate due to the dark count rate in the PMTs, of roughly 0.003, in a data-taking year of  $1.5 \times 10^7$  s. MAPP-1 is protected from collision-related backgrounds by approximately 40m of rock and concrete and the vertical veto counters in front of each section of the MAPP-1 detector.

The MAPP-mCP detector is protected from cosmic ray backgrounds by a 105 m overburden. MilliQan, by comparison, is deployed near to the CMS detector at a depth of 73m. The MoEDAL-MAPP simulation group has assessed the cosmic ray background expected in the MAPP-mCP detector to be  $(4.04 \pm 0.06) \times 10^{-5} \text{ cm}^{-2} \text{ s}^{-1}$ . This amounts to about 2 muons/s incident of the top of the MAPP-mCP veto detector, with area  $\sim 4.5 \text{ m}^2$ . This rate is inconsistent with measurements taken in the UGC1 gallery in 2018. Considering the trigger requirement for mCPs and the high efficiency of the MAPP-mCP veto system the background from uncorrelated CR muons is expected to be negligible.

The most important source of background is thought to be due to cosmic ray events with high muon multiplicity where a number of muons penetrate underground together, This has been observed, for example, by the ALICE [15] TPC with effective CR muon detection area of  $17\text{m}^2$  and 28 m rock overburden, where the corresponding Fig.s for the MAPP-mCP detector at  $4.4 \text{ m}^2$  and 105 m. The concern is that a number of particles could impinge on the detector together, increasing the probability of satisfying the mCP trigger conditions. However, the greater the multiplicity of muons impinging on the MAPP-mCP detector region, the greater the chance one of these muons would VETO the event. There are several additional factors that act to reduce this potential source of background;

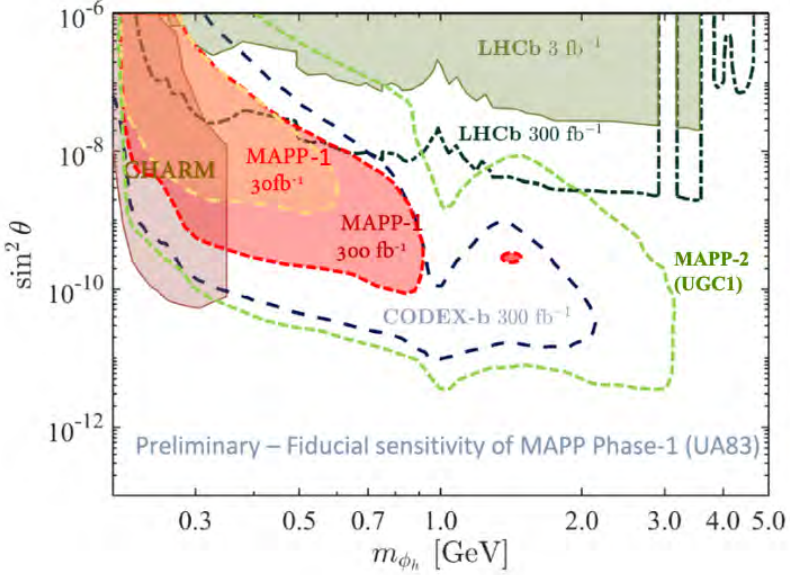


**Fig. 22:** MAPP-1 sensitivity plot for detection of a light scalar boson mixing with the Higgs boson, with three hits expected. Bounds from the CODEXb experiment are included for comparison, adapted from Fig. 3 published in Ref [16] . The exclusion bounds are shown here from the CHARM experiment considered a 400 GeV proton beam and  $2.4 \times 10^{18}$  POT [17].

- The rate of these showers is very small compared to the rate of single uncorrelated particles given above. For example, the ALICE data shows over six orders of magnitude fall in the number of events with a multiplicity of 20 muons compared to just a few muons.
- In order for cosmic ray muons from above or below to reach a bar and give even a small mCP signal the charged CR particle would normally need to cross two VETO counters which have an efficiency better than 99.7% and “clip” a bar. This would need to happen four times in four contiguous bars within the trigger time window, without hits from other CR muons in the shower registering in the VETO system;
- The rate of horizontal cosmic rays is greatly suppressed compared to the downward flux. If horizontal cosmic ray muons do reach the MAPP detector they must pass through four vertical veto walls of thickness 2.5 cm that are placed in front of MAPP and between each MAPP section, and also the back wall of the cosmic ray VETO detector of thickness 1 cm, in order to satisfy the mCP trigger;
- Neutrons associated with the muon shower can evade the VETO system and cause, for example, a nuclear recoil that can give rise to a small signal in a bar. This would need to happen in four contiguous bars within



the trigger time window. At the same time, the accompanying charged particles in the shower would have to miss the VETO system.

As stated above in Section 2 we can monitor the VETO system, with collisions-off and collisions-on, for any penetration of the VETO system. If necessary we can utilize the outer layer of scintillator bars in MAPP-mCP detector as an additional VETO system.

We can study non-beam-related background sources experimentally by running in the winter while the beam is off. In this way, we can directly register background events that mimic a signal. These runs can also be used to hone our estimates of non-beam-related backgrounds.

## 10 Future Work

Funding has been awarded by the US NSF funding body to supply additional outrigger detectors to instrument Duct-5 to further increase the acceptance of the MAPP-1 detector. The delivery dates of the scintillator and PMTs for these additional detectors are still to be exactly determined. If Duct-5 is not available for use we have a contingency plan to install them in the UA83 tunnel. This additional installation work would be the topic of a future LoI.

## 11 Conclusion

The MAPP-1 Outrigger Detector is designed to enhance the acceptance above a mCP mass of approximately  $5 \text{ GeV}/c^2$  as shown in Fig. 21 for the standard benchmark process [11][12] of DY production of mCP pairs.

The MAPP-mCP detector and Outrigger are very competitive with the milliQan detector [18] that will also be deployed for Run-3 to cover a different pseudo-rapidity range. In the event mini-charged particles are discovered by MAPP-mCP and milliQan, a signal seen in two different detectors with their different systematics would provide the necessary confirmation of a discovery. Indeed, multiple experiments to verify important experimental findings have been adopted at LEP (ALEPH, DELPHI, L3 and OPAL) and at the LHC (ATLAS and CMS).

Although MAPP-1 is designed primarily to detect feebly ionizing particles such as mCPs, it also has some useful sensitivity for neutral LLPs, as shown in Fig. 22. It could in some circumstances, provide confirmation of a signal observed by FASER [19] or vice versa. We are currently investigating using the Outrigger Detectors to enhance the sensitivity of MAPP-1 to neutral LLPs. MAPP-2, the last detector we are planning to install as part of the MoEDAL-MAPP program is designed to search for LLPs in a globally competitive way. MAPP-2 will certainly greatly enhance MoEDAL-MAPPs sensitivity to neutral LLPs compared to MAPP-1, as shown in Fig. 22.



# References

## The Bibliography

- [1] J. L. Pinfold, The MoEDAL Collaboration, “The MAPP Technical Proposal,” to be published in EPJ-ST.
- [2] 2631839 v.1 ”Derogation to IS41 MoEDAL MAPP Experiment UA83” by Fabio CORSANEGO in status: Released Link: <https://edms.cern.ch/document/2631839/1/approvalAndComments>
- [3] D. van Eijk, J. Dorant, C.Wendt, and A.Karle, “Characterization of the HZC Photonics XP82B20D and XP1805D Photomultiplier Tubes for Low-Temperature Applications,” arXiv:1904.11897v2 [physics.ins-det] 23 Jun 2019.
- [4] M. Tanabashi et al. (Particle Data Group), Review of Particle Physics,” Phys. Rev. D98, 030001 (2018).
- [5] FLUKA studies for MoEDAL installation, <https://edms.cern.ch/document/2438507/1>
- [6] Francois Butin (BE-EA), “MAPP Outrigger detector installation in UA83-LHC tunnel link ducts at LHC PT8,” EDMS NO. 2962835, approved November 1st 2023.
- [7] J. Devine, Evelyne Dho, EP Safety Group, “Assessment for the Installation of MoEDAL MAPP-mQP Detector in UGC1 gallery for the installation of the Phase-1 MAPP detector in the UGC1 gallery, EDMS NO. 2428296, Version 1.0.
- [8] [https://lhcb.web.cern.ch/Visiting\\_Pit\\_8/Access\\_request\\_guidelines.htm](https://lhcb.web.cern.ch/Visiting_Pit_8/Access_request_guidelines.htm)
- [9] K. J. Kelly and Y.-D. Tsai, “Proton Fixed-Target Scintillation Experiment to Search for Minicharged Particles,” arXiv:1812.03998v2 [hep-ph] 14 Dec 2018.
- [10] S. Banik, V.K.S. Kashyap, M.H. Kelsey, B. Mohanty, D.H. Wright, “Simulation of energy loss of fractionally charged particles using Geant4,” Nuclear Inst. and Methods in Physics Research, A 971 (2020) 164114.
- [11] B. Holdom, “Two  $U(1)$ ’s and  $\epsilon$  charge shifts”, Phys. Lett. B 166, p196-198 (1986).
- [12] A. Haas, C. s. Hill, E. Izaguirre, I. Yavin, “Looking for milli-charge particles with a new experiment at the LHC”, Phys. Lett. B746, p117-120 (2015).

- [13] H. Vogel, J. Redondo, *J. Cosmol. Astropart. Phys.* 1402, 029 (2014).
- [14] V. Mitsou, M. de Montigny, A. Mukhopadhyay, P-P Ouimet, J. Pinfold, A. Shaa and M. Staelens, “Searching for Minicharged Particles at the Energy Frontier with the MoEDAL-MAPP Experiment at the LHC,” arXiv:2311.02185v1 [hep-ph], (2023).
- [15] J. Adam et al., ALICE Collaboration, “Study of cosmic ray events with high muon multiplicity using the ALICE detector at the CERN Large Hadron Collider,” *Journal of Cosmology and Astroparticle Physics* 2016 (2016) 32.
- [16] V. V. Gligorov, S. Knapen, M. Papucci, “D. J. Robinson, Searching for Long-lived Particles: A Compact Detector for Exotics at LHCb,” *Phys. Rev. D* 97 (1) (2018) 15023.
- [17] M. W. Winkler. “Decay and detection of a light scalar boson mixing with the Higgs boson,” *Phys. Rev. D*, 99:015018, (2019).
- [18] A. Haas et al., Looking for milli-charged particles with a new experiment at the LHC, *Phys. Lett. B* 746 (2015) 117-120.
- [19] A. Ariga et al., FASER Collaboration, “FASER’s physics reach for long-lived particles”, *Phys. Rev. D* 99 no.9, 095011 (2019).

# Appendix A

## ECR for Shielding Installation

CERN  
Organisation pour la Recherche  
Scientifique et Technologique



EDMS NO.	REV.	VALIDITY
2962835	0.2	DRAFT

REFERENCE  
**LHC-X8MAPP-EC-0002**

Date: 2023-10-19

### ENGINEERING CHANGE REQUEST

## MAPP Outrigger detector installation in UA83-LHC tunnel link ducts at LHC Pt 8

#### BRIEF DESCRIPTION OF THE PROPOSED CHANGE(S):

The MoEDAL collaboration has proposed to install a new set of detectors "MAPP outrigger" in the UA83-LHC tunnel link ducts at Point 8 of the LHC.  
This document describes the changes required to accommodate the new project.

DOCUMENT PREPARED BY:  
François BUTIN – BE-EA

DOCUMENT TO BE CHECKED BY:  
James Pinfold – EP-UAT  
Richard Soluk – EP-UHC  
Eric Thomas – EP-LBO  
Markus Brugger – BE-EA  
Christelle Gaignant – BE-ASR  
Olga Beltramello – EP-DI  
Jean-Pierre Corso – EN-ACE  
Julie Coupard – EN-ACE  
Gael Girardot – EN-EL

DOCUMENT TO BE APPROVED BY:  
EATM  
IEFC  
TRES

DOCUMENT SENT FOR INFORMATION TO:  
James DEVINE, Evelyne DHO, Caterina Bertone; Alban Vieille

#### SUMMARY OF THE ACTIONS TO BE UNDERTAKEN:

[List the main actions to be undertaken]

**Note: When approved, an Engineering Change Request becomes an Engineering Change Order.**  
This document is uncontrolled when printed. Check the EDMS to verify that this is the correct version [link to use](#).

## 1. EXISTING SITUATION AND INTRODUCTION

The MoEDAL experiment has been operating jointly with LHCb at LHC Pt8 since 2010, with little impact on infrastructure, mostly due to the joint efforts of the MoEDAL and LHCb collaborations. The MoEDAL collaboration installed the MAPP detector in the UA83 gallery in 2021. Installation is still ongoing, with most of the detector elements already in place, see EDMS 2617044.

The MoEDAL collaboration has expressed the intention to install some new experimental setup in 3 ex-ventilation ducts, linking the UA83 gallery with the LHC tunnel, see ref [1] and Figure 1 and Figure 2.

The installation of these new detector elements has a number of implications for what concerns the required infrastructure and in particular the shielding impacting both the experimental area and the LHC facilities.

**The present ECR document concerns only Duct 4 to be instrumented during YETS 23-24. In case it proves successful, and depending on availability of other ducts, another ECR document will be produced accordingly.**

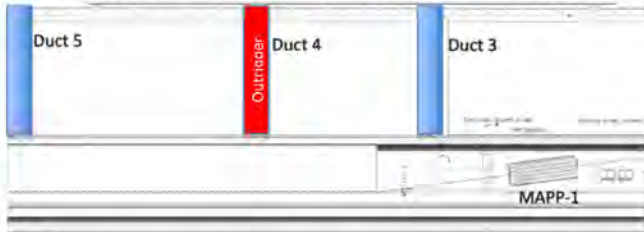


Figure 1 — Proposed location for MAPP Outrigger detectors between UA83 and LHC tunnel

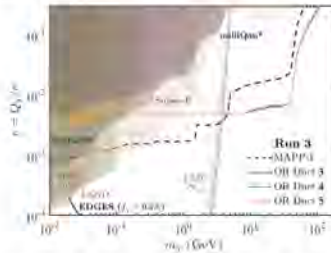


Figure 2 — Comparative simulations of MAPP Outrigger sensitivity to  $pp \rightarrow mcP^+ + mCP^-$  (via a Drell-Yan process)

## 2. REASON FOR THE CHANGE

The changes are a consequence of the evolution of the MoEDAL / MAPP 1 research programme and are intended to accommodate the evolution of the detection techniques and hardware.

## 3. DETAILED DESCRIPTION

The MAPP-1 Outrigger Detectors are proposed to be placed adjacent to the MAPP-1 detector in the duct A04L joining the beamline tunnel to the UAS3 tunnel, as shown in Figure 4.

The basic scintillator unit of the Outrigger Detector is described in Figure 3. It comprises a block of acrylic scintillator (Bicron BC-412 ) of size 60 cm x 30 cm x 5 cm readout through a light guide by a single 3.5-inch low noise PMT (HZC Photonics XP82B2FNB). This unit is assembled on a frame with another unit for insertion on a rail into the shafts that house the Outrigger detectors. This subdivision is chosen to facilitate manual handling. The units are held at an angle of 45°.

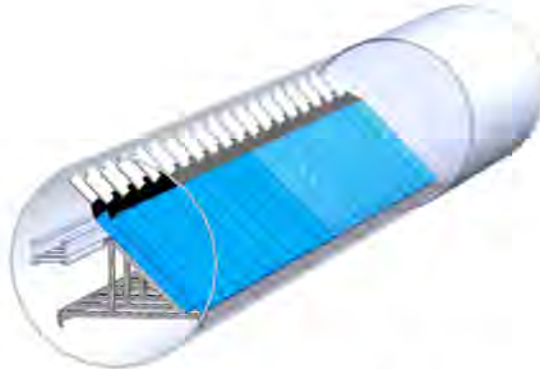


Figure 3 – Layout of the MAPP detector to be installed in A04L duct

These scintillator subunits are proposed to be installed in duct A04L joining the UAS3 tunnel to the beam tunnel. Two scintillator layers will be inserted in duct 4, as shown in Figure 3.

It is to be noted that ducts A03L, A04L and A05L are not used at this stage, nor yet planned to be used at least till L53, and have been blocked on the LHC tunnel side to



avoid circulation of possibly contaminated air from the LHC tunnel to the UA83 gallery, see Figure 4. Nevertheless, it is wished at this stage that A03L and A05L are left free in case projects emerge beyond LS3, necessitating to route cables in this region.

This position may be reconsidered at a later stage, depending on the progress of the projects.



Figure 4 — Duct for MAPP Outrigger location, seen from LHC tunnel



Figure 5 — Duct for MAPP Outrigger location, seen from UA83

In order to reduce the beam induced background in the Outrigger detectors, it is requested to install shielding equivalent to a concrete shielding plug 2 m long in the duct concerned.

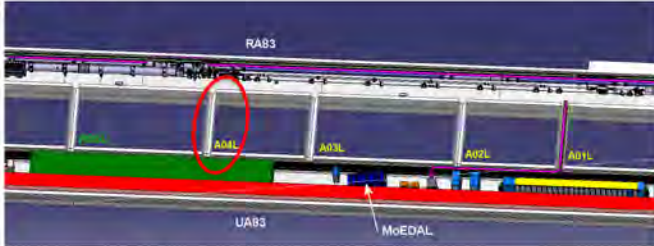


Figure 6— Duct A04L only is planned at this stage to be instrumented

In order for this shielding plug not to be permanent, it is proposed to be built out of shielding elements (iron bars and plates), that can possibly be removed at a later stage in case of need.

For ease of installation of the shielding, it will be required to remove the air-blocking panel visible on figure 4, that will be re-installed after the shielding material has been laid. 10 cm shall be left free so as to re-install this panel.

Similarly, the cable tray present in the duct will have to be removed prior to any survey or installation work can take place.

The shielding proposed for this first duct is constituted of iron bars and plates over a length of 1 m only, see Figure 7.

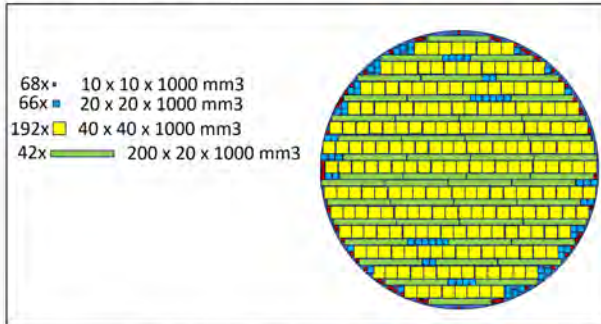


Figure 7— Filling pattern of duct A04L with iron bars



## 4. Installation schedule

A tentative installation schedule is shown in Figure 6.

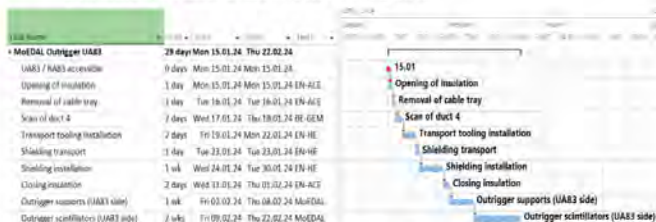


Figure 6 — Implementation schedule for the Outrigger detector and corresponding infrastructure (start date TBC)

## 5. IMPACT ON OTHER ITEMS

### 5.1 IMPACT ON UTILITIES AND SERVICES

Raw water:	No impact
Demineralized water:	No impact
Compressed air:	No impact
Electricity, cable pulling (power, signal, optical fibres...):	No impact
DEC/DIC:	Not needed
Racks (name and location):	No impact
Vacuum (bake outs, sectorisation...):	No impact
Special transport/handling:	Handling of outrigger elements will be dealt with by the collaboration (light parts). The shielding elements handling will mostly depend on the retained type.
Temporary storage of conventional/radioactive components:	No impact
Alignment and positioning:	The alignment of the Outrigger detectors will necessitate the involvement of the survey group, using the network already in place for MAPP1 detector. A scan of the ducts will be required prior to installation.
Scaffolding:	The installation of shielding and Outrigger elements may require the use of temporary scaffolding in the UAB3 gallery and/or LHC tunnel.



Controls:	No impact
GSM/WIFI networks:	No impact
Cryogenics:	No impact
Contractor(s):	The intervention of some contractors may be needed for the installation of the shielding.
Surface building(s):	No impact
Integration:	Integration drawings remain to be produced
Networks:	No impact

## 6. IMPACT ON COST, SCHEDULE AND PERFORMANCE

### 6.1 IMPACT ON COST

Detailed breakdown of the change cost:	Transport and handling	<b>5 kCHF</b>
	Shielding procurement	<b>9 kCHF</b>
	Survey / Alignment	<b>4 kCHF</b>
	Preparation /finishing work	<b>4 kCHF</b>
	Total	<b>22 kCHF</b>
Budget codes:	<b>TBC</b>	

### 6.2 IMPACT ON SCHEDULE

Proposed installation schedule:	During YETS 23-24 for duct 05, then TBC
Proposed test schedule (if applicable):	Tests will have to be performed on all safety related systems. The schedule will have to be detailed at a later stage.
Estimated duration:	The shielding installation works are expected to extend over a 2-3 weeks period. Other activities have a cumulated duration estimated to about 1 month.
Urgency:	Moderate
Flexibility of scheduling:	TBD

### 6.3 IMPACT ON PERFORMANCE

Mechanical aperture:	No impact
----------------------	-----------



Impedance:	No impact
Optics/MADX	No impact
Electron cloud (NEG coating, solenoid...)	No impact
Insulation (enamelled flange, grounding...)	No impact
Vacuum performance:	No impact
R2E impact on performance and availability:	No impact
Others:	

## 7. IMPACT ON OPERATIONAL SAFETY

The creation of a new experimental area in UGC1 has a number of consequences on the operational safety, that are detailed in Annex 2.

### 7.1 ÉLÉMENT(S) IMPORTANT(S) DE SECURITÉ

Requirement	Yes	No	Comments
EIS-Access		X	
EIS-Beam		X	
EIS-Machine		X	

### 7.2 OTHER OPERATIONAL SAFETY ASPECTS

[This chapter aims at assessing the impact of the modification during operation and maintenance of the hardware on people safety, on the environment, including access, egress, circulation and evacuation.

It doesn't concern the installation of the hardware. Worksite safety is addressed in the next chapter.]

What are the hazards introduced by the hardware?	The MAPP outrigger detector is standard assembly of equipment, each of which are used already in many other places at CERN (scintillators, photo tubes etc). A preliminary safety analysis has been performed and is available on EDM5 with number 2487833. The new hardware to be installed complies with CERN safety rules.
Could the change affect existing risk mitigation measures?	
What risk mitigation measures have to be put	



In place?	
Safety documentation to update after the modification	A safety file will have to be compiled for the MAPP Outrigger experiment.
Define the need for training or information after the change	The personnel intervening in UA83 gallery will need standard LHC tunnel safety training

## 8. WORKSITE SAFETY

[Refer to EDMS document: [1155899](#) - "Working on the CERN Site".]

### 8.1 ORGANISATION

Requirement	Yes	No	Comments
IMPACT - VIC:	X		To be organized for the various WP's
Operational radiation protection (surveys, DIMR...):		X	No ALARA classification
Radioactive storage of material:		X	None
Radioactive waste:	X		TBC if some parts of the ducts blocking material has to be evacuated
Non-radioactive waste:			None.
Fire risk/permit (IS41) (welding, grinding...):			To be checked when WP's will be described and VIC's organized.
Alarms deactivation/activation (IS37):			Not needed
Others:			

### 8.2 REGULATORY INSPECTIONS AND TESTS

Requirement	Yes	No	Responsible Group	Comments
HSE inspection of pressurised equipment:		X		
Pressure/leak tests:		X		
HSE inspection of electrical equipment:	X			The experiment will have to be inspected before HV can be switched on.
Electrical tests:		X		



Others: 

--	--	--	--

**8.3 PARTICULAR RISKS**

Requirement	Yes	No	Comments
Hazardous substances (chemicals, gas, asbestos...):		X	
Work at height:	X		Installation of equipment in the ducts may require the usage of scaffolding or PIR's
Confined space working:		X	
Noise:		X	
Cryogenic risks:		X	
Industrial X-ray (iris radia):		X	
Ionizing radiation risks (radioactive components):		X	[Traceability by IREC.]
Others:			

**9. FOLLOW-UP OF ACTIONS BY THE TECHNICAL COORDINATION**

Action	Done	Date	Comments
Carry out site activities:			
Carry out tests:			
Update layout drawings:			
Update equipment drawings:			
Update layout database:			
Update naming database:			
Update optics (MADX)			
Update procedures for maintenance and operations			
Update Safety File according to EDM5 document 1177755:			
Others:			



## 10. REFERENCES

- [1] MAPP Durtigger Technical Proposal – EDMS XXXXXX, still to be published.
- [2] Project Safety Requirement (PSR) MoEDAL MAPP and MALL detector - EDMS 2472788

# Appendix B

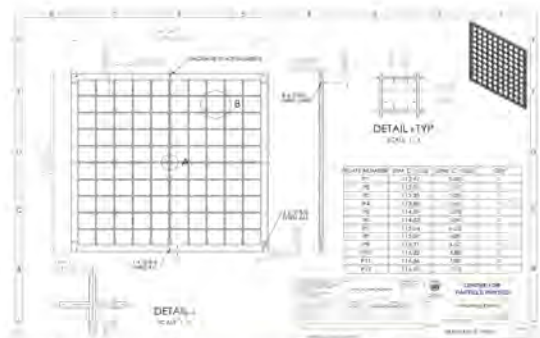
## Safety Derogation Request

EDMS 2631839 v.1 status Released access Restricted  
 PDF from EDMS\_2631839\_MoEDAL\_IS41\_derogation\_material\_fire\_v1.docx modified 2021-10-06 09:27



**HSE**  
 Occupational Health & Safety  
 and Environmental Protection Unit

<b>Safety Derogation Request Form</b>		
Date	Requested by	Dpt/Group
27 août 2021	MoEDAL- MAPP Experiment EP Safety Office	EP

<b>DESCRIPTION OF THE REQUEST</b>
<p><b>Location / Project :</b>                      UA83</p>
<p><b>Regulation related to the derogation:</b>                      Plastic materials needed for the MoEDAL Detector are not conforming to CERN IS41, and specifically needed due to their physical properties.</p>
<p><b>Brief description of the Detector :</b>                      The MAPP detector is comprised of 400 x (10 cm x 10 cm x 75 cm) scintillator bars, wrapped in Tyvek and then black tape. Each bar is connected via a short light guide to a 3-inch PMT. The bars are arranged in 4 sections, each with 100 bars with overall sensitive area of 1m<sup>2</sup>. The scintillator bars (NUVIA polystyrene based scintillator) in each section are held in a square array by three support grids made of High-Density Polyethylene (HDPE). A drawing of one of the basic HDPE support grids is shown in Figure 1. The grid separates the bars one from the other by 5m to 7 mm. The air fills the interstices between the scintillator bars.</p>
 <p style="text-align: center;"><i>Figure 1: The drawing of one of 12 HDPE support grids of the MAPP-nIQP detector.</i></p>





The weight of the scintillator in each section is supported by an aluminium T-bar support structure and a 0.5 cm aluminium plate that forms the base of each section. Additionally, each section is protected from the other by the lead-scintillator radiator plane that includes 2 x 1 mm of aluminium sheet and 5 x 2mm layers of lead. The active detector is completely encapsulated in VETO detectors comprised of 1 cm thick acrylic scintillator (Eljen-200 PVT based scintillator), with area roughly 30m<sup>2</sup>. The above arrangement is shown in Figure 2. The support structures and metal plate elements are shown in blue. The HDPS support grids and metal support structures are further emphasized in Figure 3.

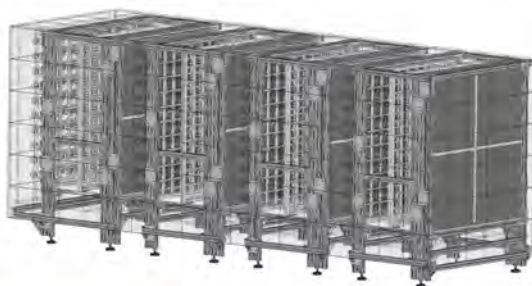


Figure 2: The basic structures of the MAPP-mQP with the outer VETO layer and the support structures emphasized.

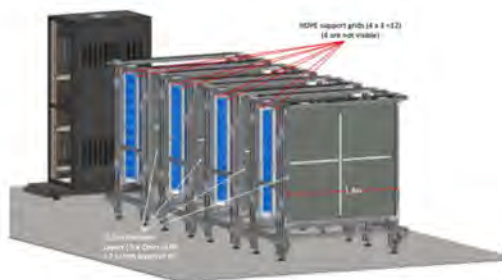


Figure 3 The basic structures of the MAPP-mQP without the outer VETO layer the support structures emphasized,

The MAPP detector and VETO layer are completely enclosed in the MAPP-mQP flame shield as shown in Figure 3. The size of the shield is roughly 1.3 x 1.5 x 4m. The flame-shield is fabricated out



of 1mm thick aluminium sheet and has a total area of  $\sim 30 \text{ m}^2$ . The aluminium encloses the plastic scintillator completely. There is no break in the flame shield for cable exit. The cables exit via a patch panel.



*Figure 4 The flame shield around the MAPP-mQP detector*

In order to provide a hermetic environment all joints in the flame shield are sealed using heavy duty aluminium tape shown in Figure 5. Any fires within the flame shield volume would be suppressed due to lack of oxygen. The slight electrical heating arising from the PMT bases within the volume of the flame shield – the only electrical elements in the region – amounts to a few hundred Watts that is dissipated by conduction and radiation from the flame shield surface

The foreseen location in UA83 is shown in Figure 5 and Figure 6 here below.



*Figure 5: Proposed location in UA83*

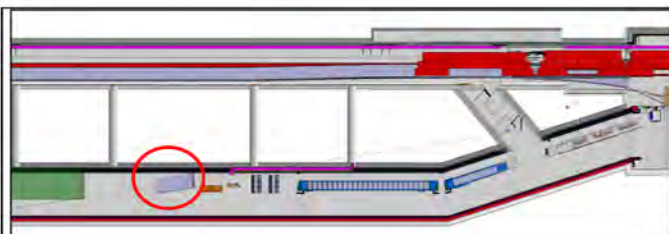


Figure 6: Proposed layout of the MAPP-mQP setup in UA83.

Further details on the materials used and other cases of applications at CERN are available in the document: **“Information Relating to Safety of the MAPP Detector With Respect to Flammability”** From J.Pinfold, available in this same EDMS node.

Further details on the installation in the UA83 are given in the ECR “LHC-X8MAPP-EC-0001 MoEDAL MAPP mQP detector in UA83” ( EDM5 2617044).



Figure 7 Heavy duty aluminium tape (0.25 mm thick), used to seal the flame shield

#### Gap compared with the reference regulation

##### Description:

Materials specifically needed for the MoEDAL Detector in virtue of their physical properties are not conforming to CERN IS 41:

Polystyrene (PS)

[https://edms.cern.ch/ui/file/2631839/1/Polystyrene\\_Material\\_Data\\_Sheet-AMCRYS.pdf](https://edms.cern.ch/ui/file/2631839/1/Polystyrene_Material_Data_Sheet-AMCRYS.pdf)



High Density Polyethylene (HDPE) <a href="https://edms.cern.ch/ui/file/2631839/1/Recycled_HDPE_Material_Safety_Data_Sheet.pdf">https://edms.cern.ch/ui/file/2631839/1/Recycled_HDPE_Material_Safety_Data_Sheet.pdf</a>	
Polyvinyl Toluene (PVT) <a href="https://edms.cern.ch/ui/file/2631839/1/EJ-200-SDS_PVT_Material_Safety_Data_Sheet.pdf">https://edms.cern.ch/ui/file/2631839/1/EJ-200-SDS_PVT_Material_Safety_Data_Sheet.pdf</a>	
<b>Cause and justification of the gap:</b> PS is required for the operation of scintillation detectors in order to perform physics in MoEDAL Experiment	
<b>Quantity :</b> (kg or m <sup>3</sup> ) 3,000 kgs of PS HDPE 326kg PVT 406kg	<b>Dimensions :</b> (length, width, diameter, thickness) PS: 10 x 10 x 75 cm / 100 units x 4 HDPE: support spacers grids --various measures described in Figure 1. PVT: set of plates, 1cm thick, total 30m <sup>2</sup>
<b>Ignition sources:</b> Low Voltage circuitry Distance to the nearest external powered system: An uninterruptible power supply, part of other LHC equipment, is at a distance ~1.5 m	
<b>Are there other previous derogation requests for the equipment/building/installation...?</b> (Not for this installation (A previous derogation has been made for MoEDAL in UX85 EDMS 893553))	
<b>What are the alternatives that have been investigated and why were they not put into place ?</b> The scintillators for the detector are housed within a flame-resistant metal casing, to prevent the propagation of fire. This mitigation is considered in the context of the derogation request required from HSE. This measure is integral to the detector and does not require any external mitigation measures. The material properties of PS are required for scintillator detectors of this type, no other alternative is possible.	
<b>Documents provided by the requestor:</b> (Click on gap here to enter text.)	

APPLICABLE SAFETY DOMAIN		
<i>(a single domain per derogation)</i>		
<input type="checkbox"/> Mechanical (pressure, lifting, machines, HVAC...)	<input type="checkbox"/> Workplace	<input type="checkbox"/> Non-ionising radiation
<input type="checkbox"/> Cryogenics	<input type="checkbox"/> Flammable gas	<input type="checkbox"/> Environmental protection
<input type="checkbox"/> Structural, civil engineering	<input type="checkbox"/> OCH	<input type="checkbox"/> Others:
<input checked="" type="checkbox"/> Fire Safety	<input type="checkbox"/> Electrical	<a href="#">Click on link here to enter text</a>
<input type="checkbox"/> Chemical	<input type="checkbox"/> Noise	



### SPECIALIST OPINION

**Specialist:**

Fabio CORSANEGO HSE-OHS-IB Jonathan Guillely HSE-OHS-PE

**Specialist opinion:**

Acceptable with the conditions agreed here below

**Compensatory measures defined in collaboration with the requestor:****safeguards: hardware/software interlocks**

power supplies are low voltage (24V), are current and temperature limited (turn off when current or temperature goes out of range) and provide an alarm signal when current or voltage moves out of some predefined operating window.

**handover of alarms generated by the system**

Three types of warning/alarm information will be provided to the CCC:

- 1) The current/voltage and temperature readings/alarms from the power supplies,
- 2) The hermetic metal flame shield is monitored by temperature sensors placed on the outside of the shield. The output of these temperature sensors will also be provided to the CCC,
- 3) There is a plan (not yet confirmed) to monitor the detectors + electronics with an IR camera whose output is provided to the CCC.

**Other safeguards:**

- 1) The power supplies, readout electronics and other non MoEDAL live equipment present in UA83 are separated by a distance of 1.5 m from the detector,
- 2) The only entities that use power in the detector volume are PMT bases. Power supplied to the bases is LV and only stopped up in the base,
- 3) The detector volume is completely encased in a hermetic (sealed to exclude air movement) flame shield. Cables enter the volume via a patch panel. Metal planes separate each of the four compartments of the detector. A strong metal plate forms the base of the scintillator bar compartments.

**Conditions for the validity of the derogation :**

- Temporary derogation - expiry date : [click on the document number](#)  
 Permanent derogation

**Description of the conditions for retaining validity:**

Observance of the conditions defined in this document

**Documents applicable to the reply:**

### TRACEABILITY

Reference and version EDMS : <https://edms.cem.ch/document/2631839/1>

### STATUS OF THE DEROGATION

See EDMS

# Appendix C

## Acrylic Safety Sheet

### Acrylite Acrylic Material Safety Data Sheet

#### 1. Chemical Product and Company Identification

##### ACRYLITE® FF Acrylic Sheet

Supplier:  
A & C Plastics, Inc.  
6135 Northdale  
Houston, TX 77087-5095

Product Information Number 1-207-490-4242  
24 Hour Emergency Number, CHEMTREC 1-800-424-9300

® is a registered trademark

Product Use: building glazing, light advertising, furniture, trade-fair booth design, displays, decoration, Industrial Use

#### 2. Composition/Information on Ingredients

This material is classified as not hazardous under OSHA regulations.

<u>Ingredients</u>	<u>CAS Reg. No.</u>	<u>Weight %</u>
acrylic copolymer	trade secret	100

NJTSR # 56705700001-6897 P

See Section 8, Exposure Controls/Personal Protection

#### 3. Hazards Identification

##### Emergency Overview

Color: colorless or colored  
Appearance: solid in various forms  
Odor: odorless

Under normal conditions of use, this product is not expected to create any unusual industrial hazards.

##### Primary Routes of Exposure

Eye contact (if exposed to chips)

##### Potential Health Effects

###### Inhalation

No hazard expected in normal use.

###### Eye Contact

No hazard expected in normal use.  
Material can cause the following:  
- mechanical irritation



## Acrylite Acrylic Material Safety Data Sheet

### Skin Contact

Material can cause the following:  
- cuts (when using cut sheets)

### Ingestion

No hazard expected in normal use.

### Potential Environmental Effects

See SECTION 12, Ecological Information

---

## 4. First Aid Measures

### First Aid Procedures

#### Inhalation

No specific treatment is necessary since this material is not likely to be hazardous by inhalation.

#### Eye Contact

If mechanical irritation occurs flush eyes thoroughly with a large amount of water, consult a physician if irritation persists. (possible during machining processes)

#### Skin Contact

No specific treatment is necessary since this material is not likely to be hazardous.

#### Ingestion

Ingestion is not considered a potential route of exposure.

---

## 5. Fire-Fighting Measures

Flash point	> 250 °C ( ASTM D1929-68 ) > 482 °F ( ASTM D1929-68 )
Autoignition Temperature	> 400 °C ( ASTM D1929-68 ) > 752 °F ( ASTM D1929-68 )

Lower explosion limit not applicable

Upper explosion limit not applicable

OSHA Flammability Classification none

### Other Flammable Properties

Use water spray to cool containers exposed to fire.

### Extinguishing Media

Use the following extinguishing media when fighting fires involving this material:  
water spray - foam - dry chemical - carbon dioxide

### Fire Fighting Procedures

As in any fire, wear self-contained breathing apparatus pressure-demand, MSHA/NIOSH (approved or equivalent) and full protective gear.





## Acrylite Acrylic Material Safety Data Sheet

### 6. Accidental Release Measures

#### Procedures

Collect material and place in a disposal container, Obey relevant local, state, provincial and federal laws and regulations.  
See Material Safety Data Sheet section 8, Exposure Controls/Personal Protection.

### 7. Handling and Storage

#### Handling

During thermal processing and/or machining local exhaust ventilation at processing machines is necessary.

#### Storage

Storage: dry.

### 8. Exposure Controls/Personal Protection

#### Exposure Limit Information

##### ACRYLIC COPOLYMER

trade secret

No Occupational Exposure Values established (ACGIH, OSHA, Canada and Mexico).

#### Engineering Controls (Ventilation)

If use operations generate dust, use adequate ventilation.

#### Respiratory Protection

A respiratory protection program meeting OSHA 1910.134 and ANSI Z88.2 requirements must be followed whenever workplace conditions warrant a respirator's use.

#### Eye Protection

goggles for machining operations

#### Hand Protection

protective gloves against mechanical risks

#### Other Protective Equipment

To identify additional Personal Protective Equipment (PPE) requirements, it is recommended that a hazard assessment in accordance with the OSHA PPE Standard (29CFR1910.132) be conducted before using this product.

### 9. Physical and Chemical Properties

Appearance	colorless or colored
Physical state	solid in various forms
Odor	odorless
Flash point	> 250 °C ( ASTM D1929-68 ) > 482 °F ( ASTM D1929-68 )
pH-value	not applicable



## Acrylite Acrylic Material Safety Data Sheet

Viscosity (dynamic)	not applicable
Specific gravity (water = 1)	1.19 g/cm <sup>3</sup> at 20 °C / 68 °F
Vapor density (air = 1)	not applicable
Vapor pressure	not applicable
Softening Temperature	approx. 102 °C / 216 °F
Boiling Temperature	not applicable
Solubility in water	Insoluble
n-Octanol/water partition coefficient	not applicable
Evaporation rate	not applicable
Odor threshold	not available
Further information	none
See Section 5, Fire Fighting Measures	

### 10. Stability and Reactivity

#### Stability

This product is stable under normal storage conditions.

#### Conditions To Avoid

This material is considered stable.

#### Incompatibility With Other Materials

Oxidizing agents. No known incompatibility with other materials.

#### Hazardous Decomposition Products

In case of thermal decomposition, combustible vapours are formed, which are irritating to eyes and respiratory system, mainly consisting of methyl methacrylate.

#### Hazardous Polymerization

Product will not undergo polymerization.

### 11. Toxicological Information

#### Further Information on Toxicology

The product has not been tested toxicologically. When handled and used as directed the product will not cause hazardous effects to health according to studies on similar products and practical experience.

### 12. Ecological Information

#### Information on Elimination (Persistence and Degradability)

##### Ecotoxicological Effect

#### Further Information on Ecology

The product has not been tested ecotoxicologically.

On the basis of the products consistency as well as its low water solubility a bio availability is unlikely. Studies on products with similar composition confirm this assumption.

## Acrylite Acrylic Material Safety Data Sheet

### 13. Disposal Considerations

#### Procedures

Waste must be disposed of in accordance with federal, state and local regulations. Incineration is the preferred method. A & C Plastics encourages the recycle, recovery and reuse of materials, where permitted, as an alternate to disposal as a waste.

### 14. Transport Information

#### Further information

Not subject to the regulations on dangerous goods.

### 15. Regulatory Information

#### INVENTORY INFORMATION

EINECS (EU)	listed or exempted
TSCA (USA)	listed or exempted
DSL (CDN)	listed or exempted

#### US FEDERAL REGULATORY INFORMATION

Component / CASRN	TPQ (lbs)	CERCLARQ (lbs) (40CFR302.4)	SARA 302 List of EHS	SARA 313 (40CFR112)	TSCA 12b <sup>1</sup>
-------------------	-----------	--------------------------------	-------------------------	------------------------	-----------------------

NONE

#### COMPONENT CLASSIFICATION UNDER CLEAN AIR ACT SECTION 112

Component / CASRN	Weight %	HAP	EHAP
-------------------	----------	-----	------

NONE

#### PRODUCT CLASSIFICATION UNDER SECTION 311/312 OF SARA (40CFR370)

NONE

#### US STATE REGULATORY INFORMATION

Component / CASRN	New Jersey RTK	Pennsylvania RTK	Massachusetts RTK	California Proposition 65 Cancer	California Proposition 65 Reproductive
-------------------	-------------------	---------------------	----------------------	--	--

acrylic polymer // trade secret	NO	NO	NO	NO	NO
------------------------------------	----	----	----	----	----

This product contains (a) chemical(s) known to the State of California to cause cancer and birth defects or other reproductive harm.

## Acrylite Acrylic Material Safety Data Sheet

### CANADIAN REGULATION

This product has been classified in accordance with the hazard criteria of the Controlled Products Regulation and the MSDS contains all information required by the Controlled Products Regulations.

This is a non-controlled product.

WHMIS: NO

Component / CASRN

NPRI

NONE

### 16. Other Information

	Health	Flammability	Physical Hazard
HMIS-Ratings	0	1	0
NFPA-Ratings	0	1	0
	<b>HMIS Hazard Ratings</b>		<b>NFPA Hazard Ratings</b>
	4 = severe		4 = extreme
	3 = serious		3 = high
	2 = moderate		2 = moderate
	1 = slight		1 = slight
	0 = minimal		0 = insignificant
	N = no rating for powders		N = no rating for powders
	* = chronic health hazard		

This MSDS was prepared in accordance with ANSI Z400.1-1998.

Places marked by || have been amended from the last version.

This information and all technical and other advice are based on A & C Plastics, Inc. present knowledge and experience. However, A & C Plastics, Inc. assumes no liability for such information or advice, including the extent to which such information or advice may relate to third party intellectual property rights. A & C Plastics, Inc. reserves the right to make any changes to information or advice at any time, without prior or subsequent notice. A & C Plastics, Inc. DISCLAIMS ALL REPRESENTATIONS AND WARRANTIES, WHETHER EXPRESS OR IMPLIED, AND SHALL HAVE NO LIABILITY FOR MERCHANTABILITY OF THE PRODUCT OR ITS FITNESS FOR A PARTICULAR PURPOSE (EVEN IF A & C Plastics, Inc. IS AWARE OF SUCH PURPOSE), OR OTHERWISE. A & C Plastics, Inc. SHALL NOT BE RESPONSIBLE FOR CONSEQUENTIAL, INDIRECT OR INCIDENTAL DAMAGES (INCLUDING LOSS OF PROFITS) OF ANY KIND. It is the customer's sole responsibility to arrange for inspection and testing of all products by qualified experts. Reference to trade names used by other companies is neither a recommendation nor an endorsement of the corresponding product, and does not imply that similar products could not be used.